Cell PRESS

Cell Host & Microbe
Article

The Ubiquitin Ligase Riplet Is Essential for RIG-I-Dependent Innate Immune Responses to RNA Virus Infection

Hiroyuki Oshiumi,[1,*] Moeko Miyashita,[1] Naokazu Inoue,[2] Masaru Okabe,[2] Misako Matsumoto,[1] and Tsukasa Seya[1]
[1]Department of Microbiology and Immunology, Graduate School of Medicine, Hokkaido University, Kita-15, Nishi-7, Kita-ku Sapporo 060-8638, Japan
[2]Research Institute for Microbial Diseases, Osaka University, 3-1 Yamadaoka, Suita, Osaka 565-0871, Japan
*Correspondence: oshiumi@med.hokudai.ac.jp
DOI 10.1016/j.chom.2010.11.008

SUMMARY

RNA virus infection is recognized by the RIG-I-like receptors RIG-I and MDA5, which induce antiviral responses including the production of type I interferons (IFNs) and proinflammatory cytokines. RIG-I is regulated by Lys63-linked polyubiquitination, and three E3 ubiquitin ligases, RNF125, TRIM25, and Riplet, are reported to target RIG-I for ubiquitination. To examine the importance of Riplet in vivo, we generated Riplet-deficient mice. Fibroblasts, macrophages, and conventional dendritic cells from Riplet-deficient animals were defective for the production of IFN and other cytokines in response to infection with several RNA viruses. However, Riplet was dispensable for the production of IFN in response to B-DNA and DNA virus infection. Riplet deficiency abolished RIG-I activation during RNA virus infection, and the mutant mice were more susceptible to vesicular stomatitis virus infection than wild-type mice. These data indicate that Riplet is essential for regulating RIG-I-mediated innate immune response against RNA virus infection in vivo.

INTRODUCTION

RNA virus infection is initially recognized by RIG-I-like receptors, RIG-I and MDA5, which induce antiviral responses such as the production of type I interferons (IFNs) and proinflammatory cytokines (Yoneyama and Fujita, 2009; Takeuchi and Akira, 2010). Analyses of RIG-I and MDA5 knockout mice showed that RIG-I is essential for type I IFN production by mouse embryonic fibroblasts (MEFs), conventional dendritic cells (cDCs), and macrophages (Mfs) in response to RNA viruses such as vesicular stomatitis virus (VSV), influenza A virus (Flu), hepatitis C virus (HCV), Sendai virus (SeV), and Japanese encephalitis virus (JEV). MDA5 is critical in picornavirus infection (Kato et al., 2006; Saito et al., 2007). However, in plasmacytoid DCs (pDCs), loss of RIG-I has no effect on viral induction of IFNs, and TLR7 and MyD88 are required for inducing immune responses in these cells (Diebold et al., 2004; Kato et al., 2005; Kumar et al., 2006; Sun et al., 2006).

RIG-I consists of two N-terminal CARDs, a central DExD/H helicase domain, and a C-terminal repressor domain (CTD) (Yoneyama et al., 2004). Before viral infection, CTD of RIG-I suppresses N-terminal CARDs (Saito et al., 2007). When the CTD of RIG-I recognizes the 5′ triphosphate-double-stranded (ds) viral RNA, the conformation of the RIG-I protein changes, and the N-terminal CARD triggers interaction with its downstream partner IPS-1 (Hornung et al., 2006; Pichlmair et al., 2006; Saito et al., 2007; Cui et al., 2008; Takahasi et al., 2008; Rehwinkel et al., 2010). IPS-1 contains an N-terminal CARD that interacts with the tandem CARDs of RIG-I and a C-terminal transmembrane domain that localizes it to the mitochondrial outer membrane (Kawai et al., 2005; Meylan et al., 2005; Seth et al., 2005; Xu et al., 2005). IPS-1 activates TBK1 kinase, which mediates phosphorylation of IRF-3, leading to its dimerization and translocation into the nucleus (Kumar et al., 2006; Sun et al., 2006). The IRF-3 dimers, NF-κB, and AP-1 transcription factors activate type I IFN transcription (Honda et al., 2005). The secreted type I IFNs activates the IFNAR, which leads to phosphorylation and nuclear translocation of STAT1 (Akira et al., 2006; Honda et al., 2006).

RIG-I is regulated by ubiquitination. Three E3 ubiquitin ligases, RNF125, TRIM25, and Riplet, target RIG-I (Arimoto et al., 2007; Gack et al., 2007; Oshiumi et al., 2009). RNF125 functions as a negative regulator for RIG-I signaling and mediates Lys48-linked polyubiquitination of RIG-I, leading to protein degradation by the proteasome (Arimoto et al., 2007). On the other hand, TRIM25 and Riplet function as positive regulators for the signaling. TRIM25 mediates Lys63-linked polyubiquitination at Lys172 of RIG-I CARDs (Gack et al., 2007). Lys63-linked polyubiquitination induces interaction between RIG-I and IPS-1 CARDs, leading to the activation of signaling (Gack et al., 2007, 2008). However, there are several reports that describe other models. First, Zeng et al. developed an in vitro reconstitution system of the RIG-I pathway (Zeng et al., 2010). Using this system, they showed that Lys172 of RIG-I CARDs is required for binding to the Lys63-linked polyubiquitin chain (Zeng et al., 2010). They postulated that polyubiquitin binding and not ubiquitin modification is required for RIG-I activation (Zeng et al., 2010). In their model, unanchored polyubiquitin chains are responsible for RIG-I activation. However, they did not rule out the possibility that ubiquitination of some signaling proteins may contribute to RIG-I activation (Zeng et al., 2010). Second, Fujita T and his colleagues reported that residue 172 of mouse RIG-I is not Lys but Gln and human RIG-I K172R mutant was normally activated by SeV infection in RIG-I KO MEFs (Shigemoto et al., 2009).

The third ubiquitin ligase, Riplet, mediates Lys63-linked polyubiquitination of RIG-I CTD and CARDs (Gao et al., 2009; Oshiumi et al., 2009). This polyubiquitination promotes RIG-I activation and its antiviral activity in human cells (Horner and Gale, 2009; Nakhaei et al., 2009; Takeuchi and Akira, 2010; Yoneyama and Fujita, 2010); however, in vivo evidence is absent. Type I IFNs are mainly produced by DCs or Mf in vivo, and RIG-I is essential for type I IFN production in cDC and Mf (Kato et al., 2005; Sun et al., 2006; Kumagai et al., 2007). The role of Riplet in these cells also has not yet been examined. Both TRIM25 and Riplet proteins mediate Lys63-linked polyubiquitination of RIG-I, and thus Gao et al. suggested that Riplet may be a complementary factor of TRIM25 for RIG-I activation (Gao et al., 2009). Therefore, it is not known whether Riplet is essential for RIG-I activation. To address these issues, we generated Riplet knockout mice. Our analysis revealed that Riplet is essential for the RIG-I activation and innate immune responses against viral infection in vivo.

RESULTS

Ubiquitous Expression of Riplet mRNA

First, we examined mouse Riplet mRNA expression by quantitative PCR (qPCR), and found it to be ubiquitously expressed in various tissues, MEFs, bone marrow-derived DCs (BM-DCs), and Mf (BM-Mf) (Figure 1A, left panel). Furthermore, we have previously shown that human Riplet mRNA is expressed in various tissues. When we examined the expression of Riplet mRNA in human DCs, it was observed in human DCs as in HeLa cells (Figure 1A, right panel). These data indicate that Riplet is expressed in various tissues and cells that are able to produce type I IFNs.

Generation of Riplet-Deficient Mice

Previously, we have shown that Riplet is a positive regulator for RIG-I-mediated signaling, and it mediates Lys63-linked polyubiquitination of RIG-I. However, the functional role of Riplet in vivo remains unclear. To investigate the role of Riplet in vivo, we generated Riplet-deficient (*Riplet*$^{-/-}$) mice by homologous recombination of embryonic stem cells (ESCs) (Figure 1B). We confirmed the target disruption of Riplet without deletion outside the targeted region (Figure 1C, and see Figures S1A and S1B available online). Riplet mRNA expression was abolished in *Riplet*$^{-/-}$ cells (Figures 1E and 1F), and the knockout of Riplet did not affect the expression of other genes, such as RIG-I, MDA5, IPS-1, TICAM-1, TLR3, and TRIM25, which are involved in type I IFN production (Figure 1F). The mutant mice were born at the Mendelian ratio from *Riplet*$^{+/-}$ parents (Figure 1D), and they developed and bred normally. These mice displayed no apparent abnormalities up to 7 months of age. Mutations in the human Riplet/RNF135 gene cause the overgrowth syndrome (Douglas et al., 2007). We did not observe any overgrowth phenotypes in *Riplet*$^{+/-}$ and *Riplet*$^{-/-}$ mice. Next, we examined the composition of CD4-, CD8-, CD11c-, and/or PDCA1-positive cells in the spleen, and found no difference between wild-type and *Riplet*$^{-/-}$ mice (Figures S1C and S1D). Induction of cDC from BM in the presence of GM-CSF was also normal in *Riplet*$^{-/-}$ mice (Figure S1E). Therefore, the mouse Riplet gene is dispensable for development.

Riplet$^{-/-}$ Embryonic Fibroblasts Are Defective in Innate Immune Responses against RNA Viruses

Riplet is a positive regulator for RIG-I-mediated signaling. In mouse fibroblast, VSV and Flu are mainly recognized by RIG-I (Kato et al., 2006). Furthermore HCV 3′UTR RNA is also recognized by RIG-I (Saito et al., 2008). Therefore, we first examined the expression of type I IFNs, IFN-inducible gene IP-10, and Ccl5 in MEFs after HCV 3′UTR dsRNA transfection or infection with VSV or Flu. The induction of mRNA of IFN-α2, -β, IP-10, and Ccl5 in response to VSV or Flu was abrogated in *Riplet*$^{-/-}$ MEFs (Figures 2A–2D). In addition, transfection of low concentration of HCV 3′UTR dsRNA (0.05–0.2 μg/well) also failed to upregulate IFN-α2, -β, and IFN-inducible genes in *Riplet*$^{-/-}$ MEFs (Figures 2A–2D).

Single-stranded (ss) RNA, which is synthesized by T7 RNA polymerase in vitro, induced lower IFN-β expression than dsRNA (Figure S2A). The induction of IFN-β mRNA by HCV 3′UTR ssRNA was also abolished in *Riplet*$^{-/-}$ MEFs (Figure S2A). Although the induction of IFN-β mRNA in response to VSV infection was abrogated in *Riplet*$^{-/-}$ MEFs even at high (moi = 5) or low multiplicities of infection (moi = 0.2 or 1), the induction of IFN-β mRNA in response to high concentration of HCV dsRNA (0.8 μg/well) was detected in *Riplet*$^{-/-}$ MEFs (Figures S2C–S2K). Therefore, RIG-I does not require Riplet function in the presence of large amounts of naked viral RNA in the cytoplasmic region.

Recently, Onoguchi et al. reported that type III IFN, IFN-λ, induction was RIG-I dependent during viral infection (Onoguchi et al., 2007). The induction of IFN-λ mRNA in response to VSV was also abrogated in *Riplet*$^{-/-}$ MEFs (Figure S2B).

Next, we examined type I IFNs or IL-6 levels in culture supernatants after viral infection or HCV 3′UTR RNA transfection (low concentration condition). The production of IFN-α, -β, and IL-6 in culture supernatants was abrogated in *Riplet*$^{-/-}$ MEFs (Figures 3A–3C). Next, we analyzed the contribution of Riplet to the antiviral response. When MEFs were infected with VSV at various mois, cytopathic effects (CPEs) were more severe in *Riplet*$^{-/-}$ than in wild-type MEFs (Figure 3D). These results demonstrate that Riplet plays a critical role in the elimination of RNA virus infection by induction of IFN responses.

Riplet Is Dispensable for the Production of Type I IFN Induced by B-DNA and HSV-1 Infection

Cytoplasmic B-form double-stranded DNA (dsDNA) stimulates the cells to induce type I IFNs and IFN-inducible genes (Ishii et al., 2006). TBK1 is required for type I IFN induction by dsDNA (Ishii et al., 2008). Although immortalized MEFs require RIG-I for type I IFNs production by dsDNA stimulation, primary MEFs do not require IPS-1, which is a RIG-I adaptor, for type I IFNs production by dsDNA (Kumar et al., 2006; Chiu et al., 2009). We examined the expression of IFN-β and IP-10 mRNA by dsDNA stimulation in primary wild-type and *Riplet*$^{-/-}$ MEFs. IFN-β and IP-10 mRNA were detected in *Riplet*$^{-/-}$ MEFs by dsDNA transfection similar to that detected in wild-type MEFs (Figures 4A and 4B).

Next, we examined IFN-β mRNA expression during infection with DNA virus, HSV-1. Wild-type and *Riplet*$^{-/-}$ MEFs were infected with HSV-1, and IFN-β mRNA expression was examined by RT-qPCR. IFN-β expression in *Riplet*$^{-/-}$ MEFs was comparable to that in wild-type MEFs (Figure 4C). Taken together, these

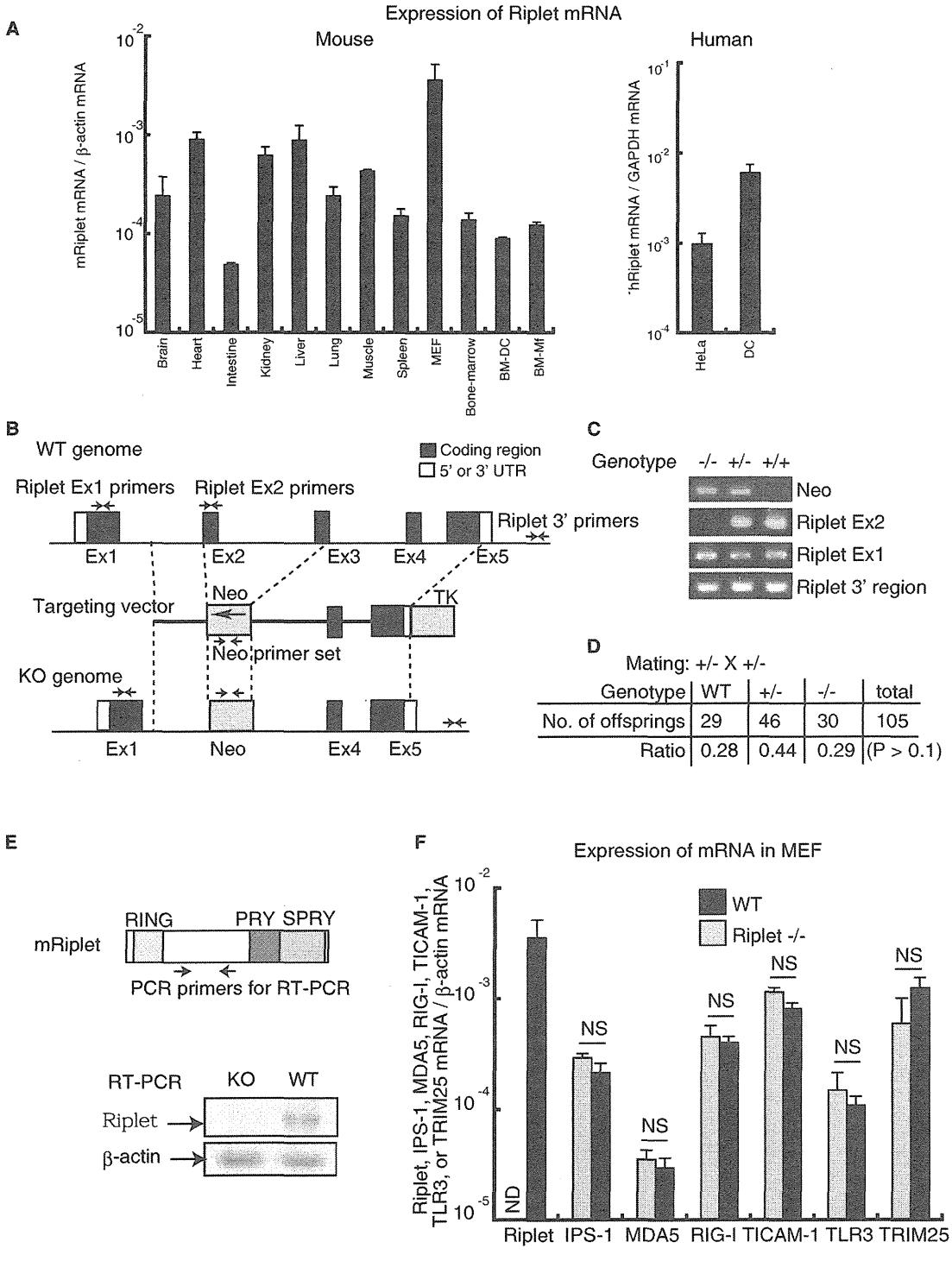

Figure 1. Targeted Disruption of the Murine Riplet Gene

(A) Riplet mRNA expression in mouse tissues and cells or human cells. RT-qPCR was performed to measure Riplet mRNA, and each sample was normalized to β-actin (mouse) or GAPDH (human). Data are shown as means ±SD and are representative of three independent experiments.

(B) Structure of the mouse Riplet gene, targeting vector, and disrupted gene. Closed boxes indicate the coding exon of Riplet, and hatched boxes indicate the Neo or TK gene coding region. The primer sets for PCR are shown by arrows.

data indicate that Riplet-dependent RIG-I activation is dispensable for type I IFN and IFN-inducible genes mRNA expression by cytoplasmic DNA in primary MEFs. This is consistent with previous studies reporting that the IPS-1-dependent pathway is dispensable for type I IFN production by cytoplasmic dsDNA stimulation (Kumar et al., 2006).

Riplet Is Essential for Triggering the RIG-I Signaling Pathway

We further examined the role of Riplet in RIG-I-mediated signaling during RNA virus infection. In RIG-I-mediated signaling, induction of type I IFNs and proinflammatory cytokines requires the activation of transcription factor IRF3. IRF3 is phosphorylated by TBK1 and IKK-ε. Phosphorylated IRF3 induces IFN-β gene expression. IFN-β produced subsequently stimulates the JAK-STAT pathway to amplify the responses. To determine the role of Riplet in signaling pathway activation, we analyzed IRF3 and STAT1 activations after VSV infection in *Riplet*$^{-/-}$ MEFs. VSV-induced dimerization of IRF3 and VSV- or Flu-induced pohsphorylation of STAT1 were abrogated in *Riplet*$^{-/-}$ MEFs (Figures 3E and 3F). These results demonstrate that Riplet is essential for activating the transcription factors that work early phase of RNA virus infection.

In the absence of viral infection, RIG-I CTD suppressed N-terminal CARDs (Saito et al., 2007). After viral infection, RIG-I CTD binds to viral RNA, leading to conformational changes (Saito et al., 2007). Later, RIG-I CARDs undergo TRIM25-mediated polyubiquitination and associate with IPS-1 CARD (Gack et al., 2007, 2008). When we tested the effect of Riplet on RIG-I activation, the full-length RIG-I protein with CTD failed to activate the IFN-β promoter in *Riplet*$^{-/-}$ MEFs (Figure 5A); however, promoter activation by the expression of RIG-I CARDs without CTD was normal in *Riplet*$^{-/-}$ MEFs (Figure 5B). These data indicate that Riplet is required for the activation of full-length RIG-I, but not for the activation of RIG-I CARDs without CTD. Next, we performed complementation assays. Immortalized *Riplet*$^{-/-}$ MEFs were transfected with an empty-, RIG-I-, or RIG-I-5KA mutant-expressing vector together with or without Riplet-expressing vector. The RIG-I-5KA mutant harbors mutations in five C-terminal Lys residues that are important for Riplet-mediated ubiquitination (Oshiumi et al., 2009). In the *Riplet*$^{-/-}$ cell line, RIG-I was not activated by HCV RNA stimulation, and Riplet expression led to the activation of wild-type RIG-I (Figure 5C). The deletion of the Riplet RING finger domain, which is the catalytic domain of ubiquitin ligase, abolished RIG-I activation (Figure 5D). Unlike wild-type RIG-I, Riplet expression failed to activate the RIG-I-5KA mutant protein (Figure 5C). The activations of wild-type and mutant RIG-I were correlated with its polyubiquitination (Figure S3A). Although the RNA binding activity was weakly reduced by the 5KA mutation, the pull-down assay showed that RIG-I-5KA mutant bound to dsRNA (Figure S3B). Next, we examined ligand-independent RIG-I activation by overexpression of Riplet. Overexpression of Riplet in HEK293 cells activated RIG-I in the absence of RIG-I ligand, such as viral RNA (Figure S3C). This ligand-independent activation of RIG-I by Riplet overexpression was also abolished by the 5KA mutation (Figure S3C). In addition, we examined the polyubiquitination of exogenously expressed RIG-I CTD fragment. Polyubiquitination of RIG-I CTD fragment was increased by overexpression of Riplet (Figure 5M), and was reduced by overexpression of the dominant-negative form of Riplet (Riplet DN) (Figure 5N). Polyubiquitination of RIG-I CTD fragment was not detected in Riplet-deficient cells (R3T cells); however, expression of Riplet led to polyubiquitination of RIG-I CTD fragment (Figure 5O). These data are consistent with our previous report (Oshiumi et al., 2009). Taken together, these data indicate that Riplet-dependent polyubiquitination of RIG-I is important for RIG-I activation.

Previously, we showed that Riplet is not involved in MDA5-mediated signaling. IFN-β promoter activation by MDA5 overexpression was normal in *Riplet*$^{-/-}$ MEFs (Figure 5E). Transfection of poly(I:C), which is recognized by MDA5, induced IFN-β, IL-6, and IP-10 expression in both wild-type and *Riplet*$^{-/-}$ MEFs (Figures 5F–5H). In addition, stimulation with lipopolysaccharide (LPS), which is a TLR4 ligand, normally induced expression of these cytokines in *Riplet*$^{-/-}$ MEFs (Figures 5I–5K). Furthermore, IL-6 production in culture medium in response to LPS was normal in *Riplet*$^{-/-}$ MEFs (Figure 5L). Taken together, these data indicate that Riplet is essential for the RIG-I-mediated type I IFN or IL-6 production upon viral infection in nonprofessional immune cells like fibroblasts, but is not required for MDA5- or TLR4-mediated signaling.

Riplet Is Required for Antiviral Innate Immune Responses in Conventional Dendritic Cells and Macrophages

We examined whether Riplet is required for the induction of type I IFN in DCs or Mf. DCs play a pivotal role in bridging innate and adaptive immune responses, and can be classified into cDCs and pDCs, the latter producing high levels of type I IFNs. Mfs also produce type I IFN. We induced cDCs from BM cells in the presence of GM-CSF (BM-DC). Twenty-four hours after VSV or Flu infection, cDCs of wild-type mice produced IFN-α, -β, and IL-6 (Figures 6A–6F). In contrast, the cDCs of *Riplet*$^{-/-}$ mice showed severely impaired IFN-α, -β, or IL-6 production during VSV or Flu infection (Figures 6A–6F). When the cDCs were stimulated with a TLR4 ligand, such as LPS, IFN-β or IL-6 production in *Riplet*$^{-/-}$ cDCs was almost normal (Figures S4A and S4B), indicating that Riplet is dispensable for LPS-induced cytokine production in cDCs.

Then we tested M-CSF-induced BM-Mf. Wild-type Mf produced IFN-α, -β, and IL-6 after VSV or Flu infection (Figures

(C) PCR of mouse tail. Genomic DNA was extracted from wild-type, *Riplet*$^{+/-}$, or *Riplet*$^{-/-}$ mice tails and PCR was performed using primers shown in (B).
(D) Genotype analyses of offspring from heterozygote intercrosses. Chi-square goodness-of-fit test indicated that deviation from Mendelian ratio was not statistically significant ($p > 0.1$).
(E) RT-PCR of MEFs. Total RNA from wild-type and *Riplet*$^{-/-}$ MEFs were extracted and subjected to RT-PCR to determine Riplet mRNA expression.
(F) Riplet, IPS-1 MDA5, RIG-I, TICAM-1, TLR3, and TRIM25 expression in MEFs. Total RNA from wild-type and *Riplet*$^{-/-}$ MEFs were extracted and subjected to RT-qPCR to determine mRNA expression. Expression of the indicated gene mRNA was normalized to β-actin mRNA expression. Data are shown as means ±SD and are representative of three independent experiments. "NS" indicates no statistically significant difference between the two samples.
See also Figure S1 and Table S1.

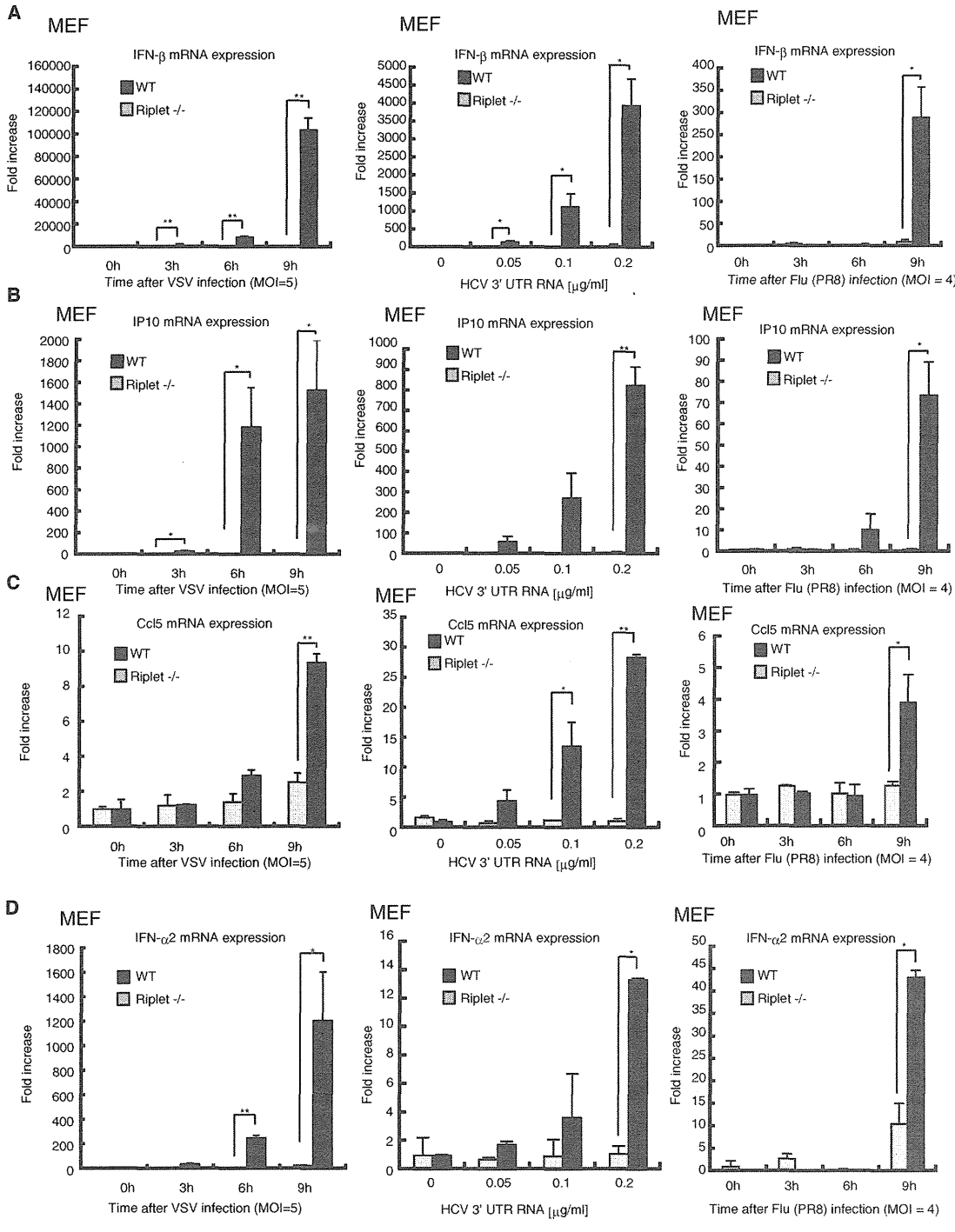

Figure 2. Abolished Responses to RNA Virus Infection in *Riplet*$^{-/-}$ Fibroblasts

Wild-type or *Riplet*$^{-/-}$ MEFs were infected with VSV or influenza A virus (Flu), and total RNA was extracted at the indicated times. Short HCV 3′UTR dsRNA was transfected into wild-type or *Riplet*$^{-/-}$ MEFs, and total RNA was extracted after 24 hr. Extracted RNA was subjected to RT-qPCR to determine IFN-β (A), IP10 (B), Ccl5 (C), or IFN-α2 (D) expression. Expression of each sample was normalized to β-actin mRNA expression. Data are shown as means ±SD and are representative of three independent experiments. *$p < 0.05$, **$p < 0.01$ (t test).

See also Figure S2 and Table S1.

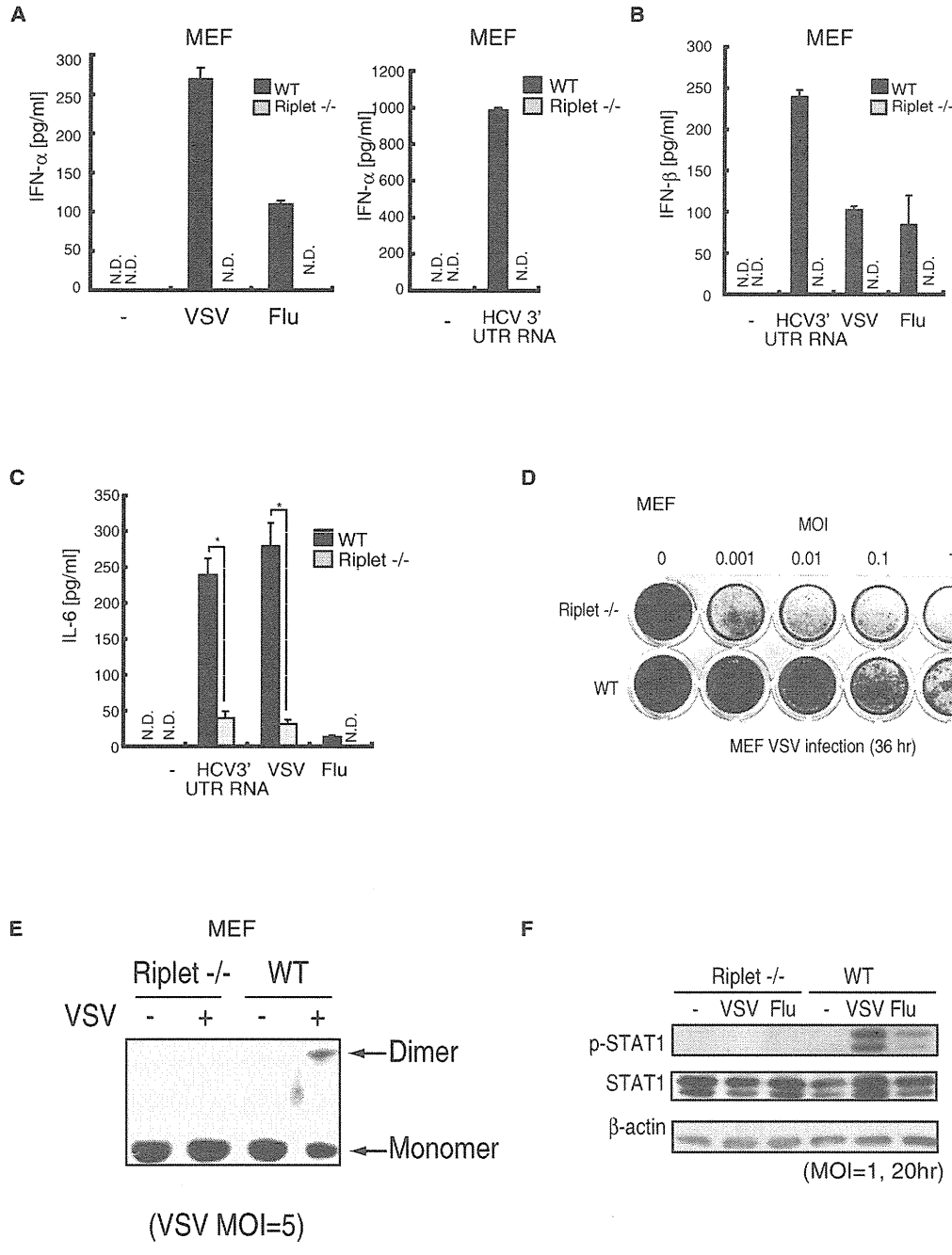

Figure 3. Role of Riplet in Antiviral Responses in Fibroblasts

(A–C) Wild-type or *Riplet*$^{-/-}$ MEFs were infected with VSV or Flu or transfected with short HCV 3′UTR dsRNA. Amounts of IFN-α (A), -β (B), and IL-6 (C) in culture supernatants were measured by ELISA after 24 hr. Data are shown as means ±SD and are representative of three independent experiments. $^{*}p < 0.05$, $^{**}p < 0.01$ (t test).

(D) Wild-type or *Riplet*$^{-/-}$ MEFs were infected with VSV at the indicated moi, and after 36 hr MEFs were fixed with formaldehyde and stained with crystal violet.

(E) Wild-type or *Riplet*$^{-/-}$ MEFs were infected with VSV at moi = 5, and after 9 hr cell lysates were prepared and analyzed by native PAGE. IRF-3 proteins were stained with anti-IRF3 antibody.

(F) Wild-type or *Riplet*$^{-/-}$ MEFs were infected with VSV or Flu at moi = 1, and after 20 hr cell lysates were prepared. The samples were analyzed by SDS-PAGE and western blotting. They were stained with anti-STAT1, phospho-STAT1, or β-actin antibodies.

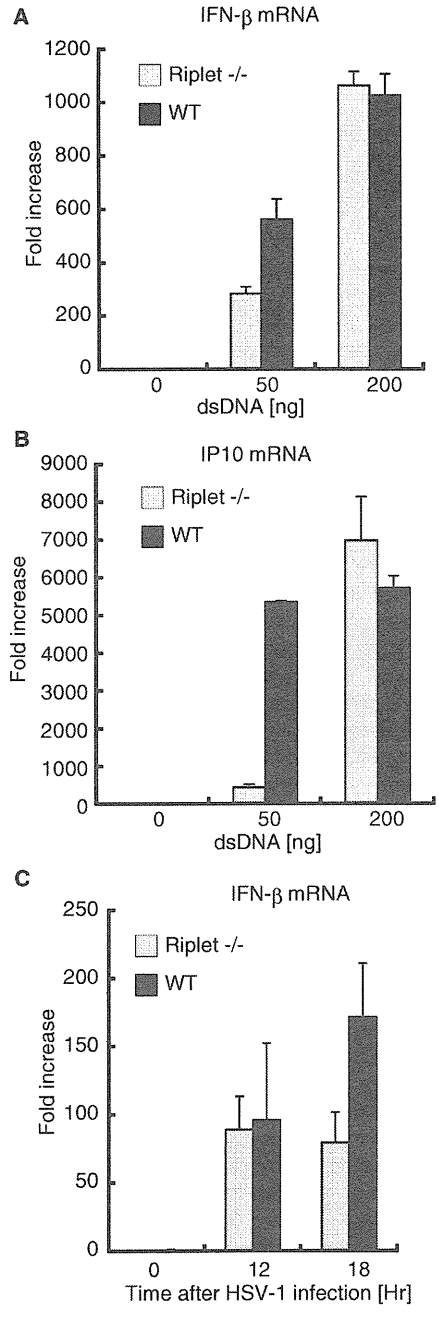

Figure 4. Role of Riplet in Type I IFN Production Induced by Cytoplasmic dsDNA

(A and B) Wild-type and *Riplet*$^{-/-}$ MEFs were transfected with the indicated amounts of dsDNA (Salomon sperm DNA) using the Lipofectamine 2000 reagent. Nine hours after the transfection, IFN-β (A) and IP-10 (B) mRNA expression was determined by RT-qPCR. Data are shown as means ±SD and are representative of three independent experiments.

(C) Wild-type and *Riplet*$^{-/-}$ MEFs were infected with HSV-1 at moi = 4, and IFN-β mRNA expression at the indicated times was examined by RT-qPCR. Data are shown as means ±SD and are representative of three independent experiments.

6A–6F). Similar to cDCs, cytokine production was reduced in Riplet knockout mice (Figures 6A–6F). Peritoneal Mf were isolated from wild-type and *Riplet*$^{-/-}$ mice. Knockout of Riplet reduced type I IFN production from peritoneal Mfs during VSV infection (Figures S4C and S4D).

We next generated Flt3L-induced DCs (Flt3L-DCs), which contain pDCs. Akira and his colleagues previously showed that the knockout of RIG-I or IPS-1 does not reduce type I IFN and IL-6 production by Flt3L-DCs, because RIG-I is dispensable for cytokine production in pDCs (Kato et al., 2005). The Flt3L-DCs of *Riplet*$^{-/-}$ mice produced normal amounts of IFN-a, -β, and IL-6 during Flu infection (Figures 6A–6F). This is consistent with the notion that Riplet is essential for the RIG-I-mediated type I IFNs and IL-6 production. Although the IFN-α levels in the culture medium after VSV infection were comparable with those in wild-type and *Riplet*$^{-/-}$ mice, Flt3L-DCs of *Riplet*$^{-/-}$ mice produced less IL-6 compared with that produced by wild-type mice through an unknown mechanism (Figure 6C).

Next, we examined type I IFN production during SeV infection. SeV infection induced IFN-α and -β productions from wild-type BM-DC, and the knockout of Riplet reduced IFN-α and -β productions from BM-DC (Figures S4E–S4J). Wild-type Flt3L-DC produced IFN-α after SeV infection, and the knockout of Riplet did not reduce IFN- α production from Flt3L-DC (Figures S4E–S4J).

Riplet Is Essential for Antiviral Immune Defense In Vivo

To investigate the role of Riplet in antiviral responses in vivo, wild-type and *Riplet*$^{-/-}$ mice were injected intraperitoneally with wild-type VSV, and sera were collected to measure type I IFN and IL-6 levels. IFN-α, -β, and IL-6 levels in sera were markedly reduced in *Riplet*$^{-/-}$ mice compared to in wild-type mice (Figures 7A and 7B, and Figure S5A). Next, wild-type and *Riplet*$^{-/-}$ mice were intranasally infected with VSV, and type I IFN levels in their sera were measured. At early time points, IFN-α and -β production was reduced in *Riplet*$^{-/-}$ mice compared to wild-type mice (Figures 7C and 7D); however, cytokine levels were comparable at later time points (Figures S5B and S5C). Previously, Ishikawa et al. observed that the knockout of STING gene, which is involved in RIG-I-dependent signaling, leads to reduction of type I IFN at early time points and relatively less reduction at later time points (Ishikawa and Barber, 2008; Ishikawa et al., 2009).

To determine if Riplet deficiency affects the survival of mice after VSV infection, the mice were intranasally infected with VSV, and their survival was monitored. Wild-type mice survived VSV infection; however, *Riplet*$^{-/-}$ mice were susceptible to VSV infection (Figure 7E). The viral titer in *Riplet*$^{-/-}$ mice brains 7 days after infection was higher than in wild-type mice (Figure 7F). These data indicate that Riplet plays a key role in the host defenses against VSV infection in vivo, and type I IFN production at early time points is important for host defenses.

DISCUSSION

In this study, we presented genetic evidence that Riplet is indispensable for antiviral responses in MEFs, BM-Mf, and BM-DCs, but not in Flt3L-DCs. The cell-type-specific requirement of Riplet

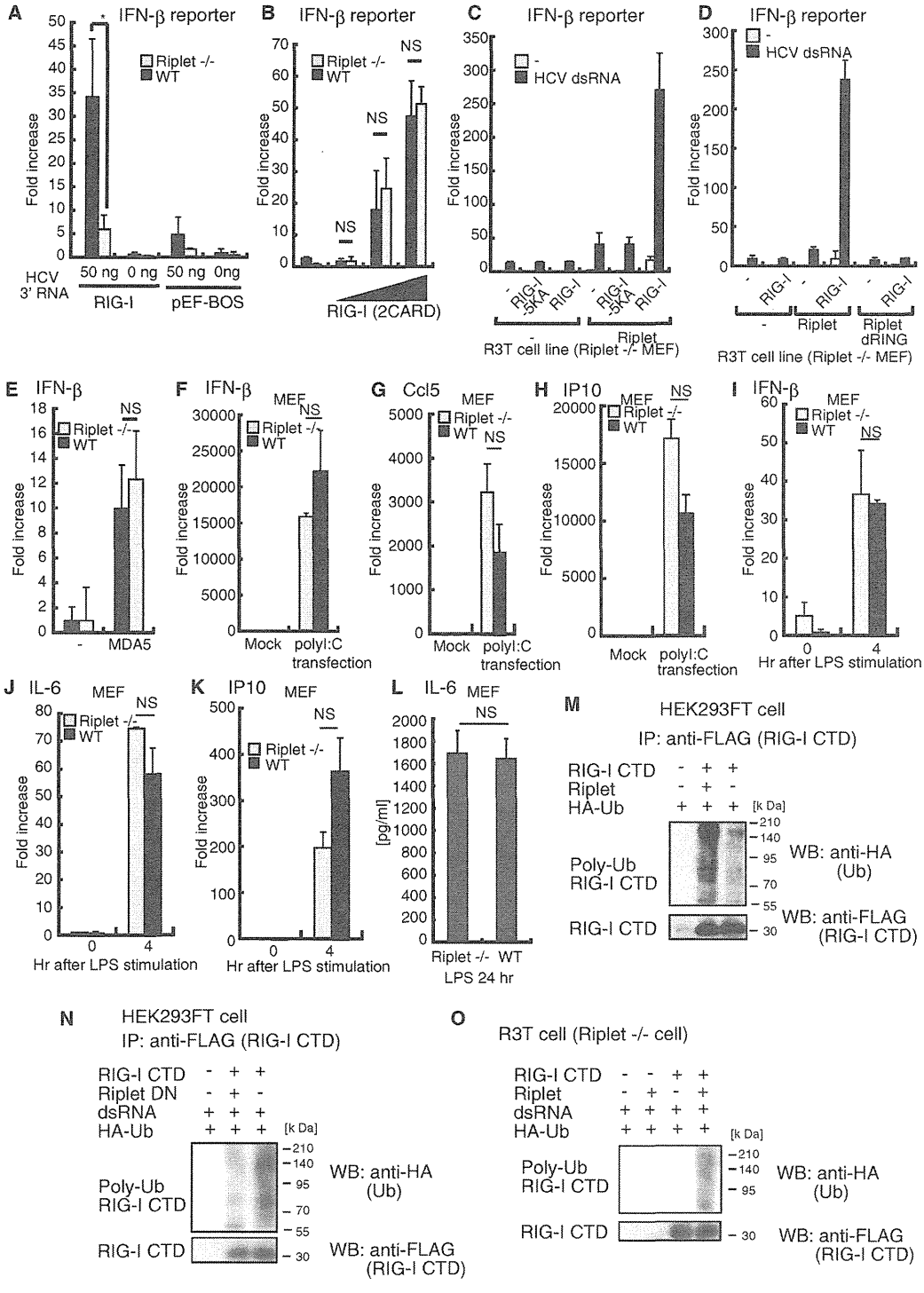

Figure 5. Role of Riplet in the RIG-I-Dependent Pathway

(A) Expression vector of full-length RIG-I and reporter plasmids were transfected into wild-type or *Riplet*$^{-/-}$ MEFs with or without HCV 3′UTR short dsRNA, and after 24 hr IFN-β promoter activation was examined by reporter gene assay. Data are shown as means ±SD and are representative of three independent experiments. *$p < 0.05$ (t test).

is similar to that of RIG-I. Previously, we showed that Riplet binds to RIG-I and mediates Lys63-linked polyubiquitination of RIG-I (Oshiumi et al., 2009). Genetic evidence in this study revealed that Riplet function is essential for RIG-I-dependent type I IFN production. Knockout of Riplet reduced type I IFN production in vivo during the early phase of VSV infection, and *Riplet*$^{-/-}$ mice were susceptible to VSV infection. Taken together, our results provide genetic evidence that Riplet is essential for RIG-I-dependent antiviral immune response in vivo. Most *RIG-I*$^{-/-}$ embryos were lethal at embryonic days 12.5–14.0 in some strain backgrounds (Kato et al., 2005). However, we could not observe any developmental defect in Riplet knockout mice as far as we examined.

Previously, Chen and his colleagues independently isolated Riplet and named it REUL (Gao et al., 2009). They reported that REUL/Riplet binds to RIG-I CARDs but not to CTD (Gao et al., 2009). Furthermore, they reported that REUL/Riplet mediates Lys63-linked polyubiquitination of Lys172 of RIG-I CARDs in a manner similar to TRIM25 (Gack et al., 2007; Gao et al., 2009). Although they did not show any expression profile data for Riplet and TRIM25, they mentioned that TRIM25 and Riplet have different distribution patterns, and thus hypothesized that REUL/Riplet is a complementary factor of TRIM25 and is required for RIG-I activation in cells that do not express TRIM25 (Gao et al., 2009). However, our genetic evidence is not consistent with their hypothesis, because Riplet is essential for RIG-I activation in MEFs that express TRIM25. Previously, Gack et al. showed that knockout of TRIM25 alone abolished RIG-I activation in MEFs (Gack et al., 2007). Therefore, null mutation in either Riplet or TRIM25 abolishes RIG-I activation. This genetic evidence indicates that Riplet can mediate polyubiquitination of RIG-I Lys residues that are not ubiquitinated by TRIM25. This means that Riplet functions differently than TRIM25 in RIG-I activation.

We isolated Riplet cDNA by yeast two-hybrid screening using the C-terminal region of RIG-I (Oshiumi et al., 2009). Because the yeast genome does not encode RIG-I, the interaction indicates the direct binding of Riplet to the RIG-I C-terminal region. The interaction between RIG-I CTD and Riplet has also been confirmed by immunoprecipitation assays in human cells (Oshiumi et al., 2009). Moreover, we have shown that Riplet expression leads to Lys63-linked polyubiquitination of RIG-I CTD (Oshiumi et al., 2009). Recently, Zheng et al. showed that RIG-I CARDs has the ability to bind to polyubiquitin chains (Zeng et al., 2010). We have carefully detected Riplet-mediated polyubiquitination of RIG-I C-terminal region without CARDs, under high-salt conditions, in which many protein-protein interactions were abolished (Oshiumi et al., 2009). Therefore, we proposed the hypothesis that Riplet mediates Lys63-linked polyubiquitination of RIG-I CTD (Oshiumi et al., 2009). This model can explain the genetic evidence that Riplet is essential for RIG-I activation in MEFs that express TRIM25. Gack et al. showed that K172R mutation alone caused near-complete loss of ubiquitination of the human RIG-I CARDs (Gack et al., 2007). Because residue 172 of mouse RIG-I is not Lys but Gln (Shigemoto et al., 2009), Riplet/Reul does not ubiquitinate residue 172 of mouse RIG-I. Based on the previous studies and our current data, we prefer the interpretation that Riplet activates RIG-I through polyubiquitination of RIG-I CTD. However, this interpretation does not exclude the possibility that Riplet ubiquitinates both CTD and CARDs of RIG-I (Gao et al., 2009; Oshiumi et al., 2009).

Previously, we showed that Lys849, -851, -888, -907, and -909 are critical residues in Riplet-mediated RIG-I CTD ubiquitination (Oshiumi et al., 2009). These five Lys residuse are close to the dsRNA binding sites of RIG-I CTD (Takahasi et al., 2008), and the 5KA mutation weakly reduced RNA binding activity of RIG-I. Therefore, it is possible that the 5KA mutation abrogate activation and polyubiquitination of RIG-I by reducing RNA biding activity of RIG-I. However, this possibility is weakened by following observations. First, the 5KA mutation caused near-complete loss of RIG-I activation, but the RIG-I-5KA mutant protein still possessed RNA binding activity. Second, overexpression of Riplet led to RIG-I activation in the absence of dsRNA in HEK293 cells, and this ligand-independent activation of RIG-I

(B) Expression vector for the two RIG-I N-terminal CARDs were transfected into wild-type or *Riplet*$^{-/-}$ MEFs together with reporter plasmids, and IFN-β promoter activation was examined by the reporter gene assay. Data are shown as means ±SD and are representative of three independent experiments. "NS" indicates not statistically significant.

(C) Empty, wild-type RIG-I-, or RIG-I-5KA mutant-expressing vectors were transfected into the *Riplet*$^{-/-}$ MEF cell line together with or without the Riplet-expressing vector. Cells were stimulated with HCV 3′UTR short dsRNA, and reporter gene assay was performed as described in (A).

(D) Empty or wild-type RIG-I-expressing vectors were transfected into the *Riplet*$^{-/-}$ MEF cell line together with empty, wild-type Riplet, or Riplet mutant (Riplet dRING)-expressing vector. Cells were stimulated with HCV 3′UTR short dsRNA, and the reporter gene assay was performed as described in (A).

(E) Empty or MDA5-expressing vectors was transfected into wild-type or *Riplet*$^{-/-}$ MEFs together with reporter plasmids, and after 24 hr IFN-β promoter activation was examined by the reporter gene assay.

(F–H) Of poly(I:C), 0.8 μg was transfected into wild-type or *Riplet*$^{-/-}$ MEFs. Twenty-four hours after transfection, total RNA was extracted from MEFs and subjected to RT-qPCR to determine IFN-β (F), Ccl5 (G), and IP10 (H) expression. Expression in each sample was normalized to the β-actin mRNA expression.

(I–K) Wild-type or *Riplet*$^{-/-}$ MEFs were stimulated with 1 μg of LPS. Total RNA was extracted at the indicated times and subjected to RT-qPCR analysis for of IFN-β (I), IL-6 (J), or IP-10 (K) expression.

(L) Wild-type or *Riplet*$^{-/-}$ MEFs were stimulated with LPS, and after 24 hr the amount of IL-6 in culture supernatants was measured by ELISA.

(M) HEK293FT cells were transfected with Riplet, FLAG-tagged RIG-I-CTD, and HA-tagged ubiquitin (HA-Ub) expression vectors. Twenty-four hours after transfection, cell lysates were extracted and immunoprecipitation was carried out with anti-FLAG antibody as previously described (Oshiumi et al., 2009). The samples were analyzed by SDS-PAGE, and western blotting was performed using anti-HA polyclonal antibody (Ub) and anit-Flag M2 monoclonal antibody (RIG-I-CTD). The plasmids are described previously (Oshiumi et al., 2009).

(N) Expression vector of dominant negative form of Riplet (Riplet DN) was transfected into HEK293FT cells together with expression vector of FLAG-tagged RIG-I CTD and HA-tagged ubiquitin. Cells were stimulated with dsRNA. Ubiquitination of RIG-I CTD was detected as in (M).

(O) R3T cells were transfected with Riplet, FLAG-tagged RIG-I-CTD, and HA-tagged ubiquitin (HA-Ub) expression vectors. Cells were stimulated with dsRNA. Ubiquitination of RIG-I-CTD was detected as in (M).

See also Figure S3.

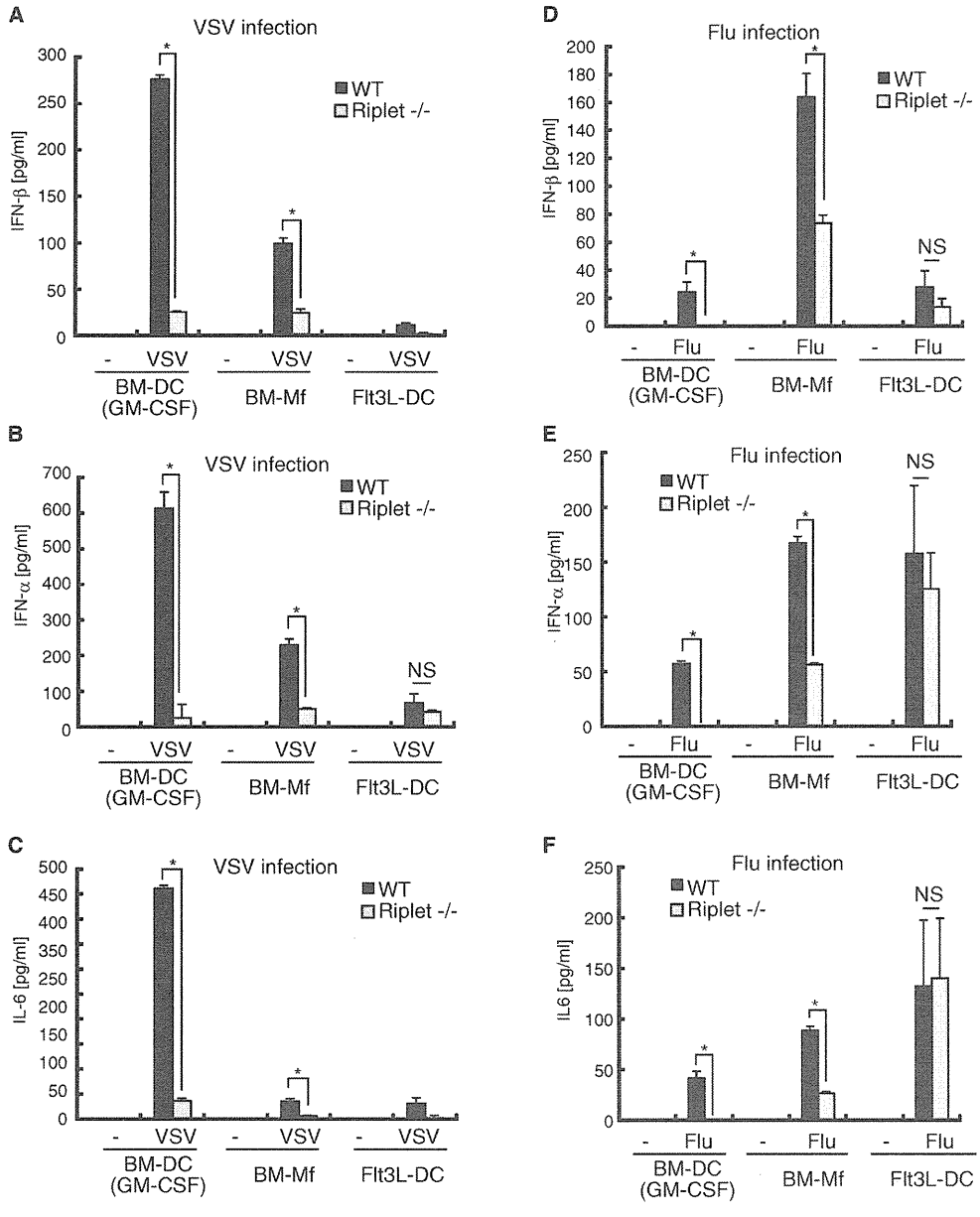

Figure 6. Role of Riplet in Responses to VSV or Flu Infection in Bone Marrow-Derived Cells

GM-DCs, BM-Mf, or Flt3L-DCs were induced from BM-derived cells in the presence of GM-CSF, M-CSF, or Flt3L and infected with VSV or influenza A virus at moi = 1. Twenty-four hours after viral infection, amounts of IFN-β (A and D), -α (B and E), and IL-6 (C and F) in culture supernatants were measured by ELISA. Data are shown as means ±SD and are representative of two independent experiments. *$p < 0.05$ (Student's t test). NS indicates not statistically significant.
See also Figure S4.

by overexpression of Riplet was also abolished by the 5KA mutation. These data support our model. However, we do not exclude the possibility that other Lys residues of RIG-I are ubiquitinated by Riplet, because we have not yet directly detected polyubiquitinated residues of RIG-I CTD by mass spectrometory analysis. Further in vitro studies are required to determine the polyubiquitination sites and to reveal precise RIG-I regulatory mechanisms by Riplet-mediated Lys63-linked polyubiquitation.

In general, E3 ubiquitin ligase targets several types of proteins. Therefore, it is possible that Riplet targets other proteins. Previous work has shown that Riplet binds to the Trk-fused gene (TFG) protein (Suzuki et al., 2001). The TFG protein interacts with TANK and NEMO, which are involved in the NF-κB pathway (Miranda et al., 2006). Although NEMO is involved in IPS-1-mediated signaling, RIG-I CARDs- or MDA5-mediated signaling was normal in *Riplet*$^{-/-}$ MEFs. Therefore, interaction between Riplet

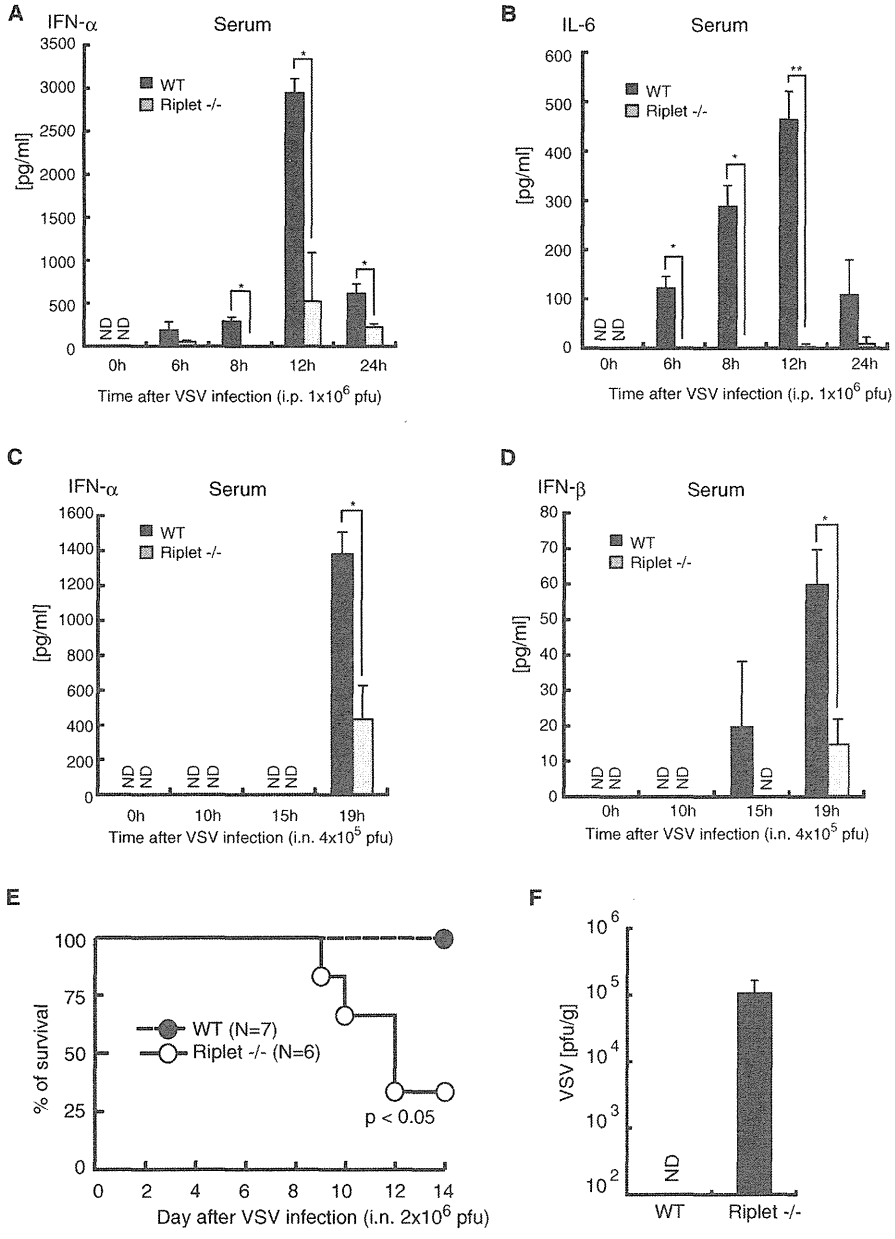

Figure 7. Role of Riplet in Antiviral Responses In Vivo

(A and B) Wild-type or *Riplet*$^{-/-}$ mice were injected intraperitoneally with 1 × 10^6 pfu of VSV. Amounts of IFN-α (A) and IL-6 (B) in mouse serum were measured by ELISA. Data are shown as mean ±SD of samples obtained from three wild-type and three Riplet −/− mice at each time point. *$p < 0.05$ (Student's t test). "ND" indicates not detected.

(C and D) Wild-type and *Riplet*$^{-/-}$ mice were infected intranasally with 4 × 10^5 pfu of VSV. Amounts of IFN-α (C) and IFN-β (D) in mouse serum were measured by ELISA.

(E) Wild-type and *Riplet*$^{-/-}$ mice were infected intranasally with 2 × 10^6 pfu of VSV and mice mortality was observed for 14 days (*$p < 0.05$ between wild-type and *Riplet*$^{-/-}$ mice, log rank test).

(F) Wild-type and *Riplet*$^{-/-}$ mice were infected intranasally with 2 × 10^6 pfu of VSV, and sacrificed for their tissues on day 7 after infection. Titers in brain were determined by the plaque assay. Viral titers in brains of wild-type mice were below 100 pfu/g, and thus not detected (ND). Data are shown as means ±SD (n = 3). See also Figure S5.

and TFG protein is not required for RIG-I-mediated signaling. However, since TFG is involved in tumorigenesis (Miranda et al., 2006), Riplet may be involved in human tumorigenesis.

Several viral proteins inhibit RIG-I-mediated signaling. For example, Flu NS1 inhibits TRIM25 and HCV NS3/4A cleaves IPS-1 (Meylan et al., 2005; Gack et al., 2009). Therefore, Riplet may be inhibited by viral proteins. Indeed, our pilot study indicated that the Riplet protein is disrupted in human hepatocyte cell lines carrying a full-length HCV replicon. RIG-I is involved in innate immune responses against various viruses. In this study, we showed that Riplet is required for innate immune responses against VSV, Flu, and SeV. Therefore, Riplet is also expected to be involved in innate immune responses against other viruses that are recognized by RIG-I.

EXPERIMENTAL PROCEDURES

Generation of Riplet-Deficient Mice

The Riplet gene was amplified by PCR using genomic DNA extracted from ESCs by PCR. The targeting vector was constructed by replacing the second and third exons with a neomycine-resistance gene cassette (Neo), and a herpes simplex virus thymidine kinase (HSV-TK) driven by PGK promoter was inserted into the genomic fragment for negative selection. After the targeting vector was transfected into 129/Sv mice-derived ESCs, G418 and gancyclovir doubly resistant colonies were selected and screened by PCR. The targeted cell line was injected in C57BL/6 blastocysts, resulting in the birth of male chimeric mice. These mice were then crossed with 129/Sv mice to obtain heterozygous mutants. The heterozygous mutants were intercrossed to obtain homozygous *Riplet*$^{-/-}$ mice.

Cells, Viruses, and Reagents

Wild-type and *Riplet*$^{-/-}$ MEFs were prepared from day 12.5–13.5 embryos. *Riplet*$^{-/-}$ MEFs were immortalized with large T antigen and named R3T cell line. BM cells were prepared from 5- to 10-week-old mice. VSV Indiana strain was provided by A. Takada (Hokkaido University). VSV was amplified using Vero cells and the viral titer was determined by the plaque assay. Flu (PR8 strain) and SeV (HVJ strain) was provided by Y. Sakoda (Hokkaido University). HSV-1 strain was provided by K. Kondo (The JIKEI University). Anti-mouse IRF3 antibody was purchased from Zymed. Anti-phospho-STAT1 antibody was purchased from Cell Signaling and anti-STAT1 antibody from Santa Cruz. Salomon sperm dsDNA was purchased from Invitrogen. To determine the viral titer in the brain, the mice were sacrificed, and the brain was aseptically removed and frozen at −80°C. The brain was homogenized in 1 ml of PBS on ice, and the titer was determined by plaque assay.

Preparation of Viral Double-Stranded RNA

cDNA of the HCV 3′UTR region was amplified from total RNA of the HCV genotype 1b full-length replicon using primers HCV-F1 and HCV-R1, and then cloned in the pGEM-T Easy Vector. The primer set sequences were HCV-F1, CTCCAGGTGAGATCAATAGG; and HCV-R1, CGTGACTAGGGCTAAGATGG. RNA was synthesized using T7 and SP6 RNA polymerases. Template DNA was digested by DNase I, and RNA was purified using TRIZOL (Invitrogen) according to manufacturer's instructions.

Quantitative PCR

For qPCR, total RNA was extracted with TRIZOL (Invitrogen) and 0.5 μg of RNA was reverse-transcribed using the High Capacity cDNA Transcription Kit (ABI) with random primers according to the manufacturer's instructions. qPCR was performed using the Step One Real-Time PCR system (ABI). Primer sequences used for qPCR are listed in Table S1.

Measurement of Cytokines

In brief, 5 × 10^5 cells in a 24-well plate were either infected with VSV or Flu, stimulated with LPS, or transfected with HCV 3′UTR dsRNA or poly(I:C). Twenty-four hours after infection, stimulation, or transfection, culture supernatants were collected and analyzed for IFN-α, -β, and IL-6 production by ELISA. Cytokine levels were measured in mouse serum obtained from the mouse tail vein. ELISA kits for mouse IFN-α and -β were purchased from PBL Biomedical Laboratories. ELSA kit for mouse IL-6 was purchased from Invitrogen.

Preparation of Dendritic Cells and Macrophages

BM cells were prepared from the femur and tibia. The cells were cultured in RPMI1640 medium supplemented with 10% FCS, 100 μM 2-Me, and 100 ng/ml human Flt3 ligand (Pepro Tech), and 10 ng/ml murine GM-CSF or culture supernatant NIH 3T3 expressing M-CSF. After 6 days, cells were collected and used as Flt3L-DC, GM-DC, or BM-Mf. In the case of GM-DC or BM-Mf, the medium was changed every 2 days.

Native PAGE Analysis

Approximately 1 × 10^6 MEFs were infected with VSV at moi = 1 for 9 hr and then lysed. Cell lysates in native PAGE sample buffer (62.5 mM Tris-HCl [pH 6.8], 15% glycerol, and BPB) were separated using native PAGE and then immunoblotted with anti-murine IRF3 antibody (Zymed).

Luciferase Assay

Expression plasmids for mouse RIG-I N-terminal CARDs, full-length RIG-I, or full-length MDA5 were constructed in pEF-BOS. The cDNA fragment encoding the ORF of RIG-I or MDA5 was amplified by RT-PCR using total RNA prepared from MEFs. The Riplet dRING mutant protein lacks 1–69 aa region. Wild-type and mutant (Riplet dRING) Riplet-expression vectors were described previously (Oshiumi et al., 2009). Wild-type or *Riplet*$^{-/-}$ MEFs were transiently transfected in 24-well plates with reporter constructs containing the IFN-β promoter and Renilla luciferase (internal control) together with the empty vector (control), RIG-I CARDs, full-length RIG-I, or MDA5 expression vectors. Twenty-four hours after transfection, cells were lysed and subjected to the luciferase assay using the Dual-Luciferase Reporter Assay system (Promega).

Statistical Analyses

Statistical significance of differences between groups was determined by the Student's t test, and survival curves were analyzed by the log rank test using Prism 4 for Macintosh software (GraphPad Sofware, Inc.). Chi-square goodness-of-fit tests and Student's t tests were performed using MS-Excel software and a chi-square distribution table.

SUPPLEMENTAL INFORMATION

Supplemental Information includes five figures, one table, and Supplemental Experimental Procedures and can be found with this article at doi:10.1016/j.chom.2010.11.008.

ACKNOWLEDGMENTS

We thank Dr. John P. Atkinson (Washington University) and Dr. Ralph Steinman (Rockefeller University) for critical discussions, Yoko Esaki and Kiyo Kawata for technical support in generating Riplet KO mice, N. Irie for a pilot study of B-DNA stimulation assay, and Sakoda Y. for technical instructions for the experiments using Flu and SeV. This work was supported in part by the Mitsubishi Foundation; Mochida Foundation; Akiyama Life Science Foundation; and Grants-in-Aid from Ministry of Education, Science, and Culture and Ministry of Health, Labor, and Welfare of Japan.

Received: June 4, 2010
Revised: August 18, 2010
Accepted: November 5, 2010
Published: December 15, 2010

REFERENCES

Akira, S., Uematsu, S., and Takeuchi, O. (2006). Pathogen recognition and innate immunity. Cell *124*, 783–801.

Arimoto, K., Takahashi, H., Hishiki, T., Konishi, H., Fujita, T., and Shimotohno, K. (2007). Negative regulation of the RIG-I signaling by the ubiquitin ligase RNF125. Proc. Natl. Acad. Sci. USA *104*, 7500–7505.

Chiu, Y.H., Macmillan, J.B., and Chen, Z.J. (2009). RNA polymerase III detects cytosolic DNA and induces type I interferons through the RIG-I pathway. Cell *138*, 576–591.

Cui, S., Eisenacher, K., Kirchhofer, A., Brzozka, K., Lammens, A., Lammens, K., Fujita, T., Conzelmann, K.K., Krug, A., and Hopfner, K.P. (2008). The C-terminal regulatory domain is the RNA 5′-triphosphate sensor of RIG-I. Mol. Cell *29*, 169–179.

Diebold, S.S., Kaisho, T., Hemmi, H., Akira, S., and Reis e Sousa, C. (2004). Innate antiviral responses by means of TLR7-mediated recognition of single-stranded RNA. Science *303*, 1529–1531.

Douglas, J., Cilliers, D., Coleman, K., Tatton-Brown, K., Barker, K., Bernhard, B., Burn, J., Huson, S., Josifova, D., Lacombe, D., et al. (2007). Mutations in RNF135, a gene within the NF1 microdeletion region, cause phenotypic abnormalities including overgrowth. Nat. Genet. *39*, 963–965.

Gack, M.U., Shin, Y.C., Joo, C.H., Urano, T., Liang, C., Sun, L., Takeuchi, O., Akira, S., Chen, Z., Inoue, S., and Jung, J.U. (2007). TRIM25 RING-finger E3 ubiquitin ligase is essential for RIG-I-mediated antiviral activity. Nature *446*, 916–920.

Gack, M.U., Kirchhofer, A., Shin, Y.C., Inn, K.S., Liang, C., Cui, S., Myong, S., Ha, T., Hopfner, K.P., and Jung, J.U. (2008). Roles of RIG-I N-terminal tandem CARD and splice variant in TRIM25-mediated antiviral signal transduction. Proc. Natl. Acad. Sci. USA *105*, 16743–16748.

Gack, M.U., Albrecht, R.A., Urano, T., Inn, K.S., Huang, I.C., Carnero, E., Farzan, M., Inoue, S., Jung, J.U., and Garcia-Sastre, A. (2009). Influenza A virus NS1 targets the ubiquitin ligase TRIM25 to evade recognition by the host viral RNA sensor RIG-I. Cell Host Microbe *5*, 439–449.

Gao, D., Yang, Y.K., Wang, R.P., Zhou, X., Diao, F.C., Li, M.D., Zhai, Z.H., Jiang, Z.F., and Chen, D.Y. (2009). REUL is a novel E3 ubiquitin ligase and stimulator of retinoic-acid-inducible gene-I. PLoS ONE *4*, e5760. 10.1371/journal.pone.0005760.

Honda, K., Yanai, H., Takaoka, A., and Taniguchi, T. (2005). Regulation of the type I IFN induction: a current view. Int. Immunol. *17*, 1367–1378.

Honda, K., Takaoka, A., and Taniguchi, T. (2006). Type I interferon [corrected] gene induction by the interferon regulatory factor family of transcription factors. Immunity *25*, 349–360.

Horner, S.M., and Gale, M., Jr. (2009). Intracellular innate immune cascades and interferon defenses that control hepatitis C virus. J. Interferon Cytokine Res. *29*, 489–498.

Hornung, V., Ellegast, J., Kim, S., Brzozka, K., Jung, A., Kato, H., Poeck, H., Akira, S., Conzelmann, K.K., Schlee, M., et al. (2006). 5′-Triphosphate RNA is the ligand for RIG-I. Science *314*, 994–997.

Ishii, K.J., Coban, C., Kato, H., Takahashi, K., Torii, Y., Takeshita, F., Ludwig, H., Sutter, G., Suzuki, K., Hemmi, H., et al. (2006). A Toll-like receptor-independent antiviral response induced by double-stranded B-form DNA. Nat. Immunol. *7*, 40–48.

Ishii, K.J., Kawagoe, T., Koyama, S., Matsui, K., Kumar, H., Kawai, T., Uematsu, S., Takeuchi, O., Takeshita, F., Coban, C., and Akira, S. (2008). TANK-binding kinase-1 delineates innate and adaptive immune responses to DNA vaccines. Nature *451*, 725–729.

Ishikawa, H., and Barber, G.N. (2008). STING is an endoplasmic reticulum adaptor that facilitates innate immune signalling. Nature *455*, 674–678.

Ishikawa, H., Ma, Z., and Barber, G.N. (2009). STING regulates intracellular DNA-mediated, type I interferon-dependent innate immunity. Nature *461*, 788–792.

Kato, H., Sato, S., Yoneyama, M., Yamamoto, M., Uematsu, S., Matsui, K., Tsujimura, T., Takeda, K., Fujita, T., Takeuchi, O., and Akira, S. (2005). Cell type-specific involvement of RIG-I in antiviral response. Immunity *23*, 19–28.

Kato, H., Takeuchi, O., Sato, S., Yoneyama, M., Yamamoto, M., Matsui, K., Uematsu, S., Jung, A., Kawai, T., Ishii, K.J., et al. (2006). Differential roles of MDA5 and RIG-I helicases in the recognition of RNA viruses. Nature *441*, 101–105.

Kawai, T., Takahashi, K., Sato, S., Coban, C., Kumar, H., Kato, H., Ishii, K.J., Takeuchi, O., and Akira, S. (2005). IPS-1, an adaptor triggering RIG-I- and Mda5-mediated type I interferon induction. Nat. Immunol. *6*, 981–988.

Kumagai, Y., Takeuchi, O., Kato, H., Kumar, H., Matsui, K., Morii, E., Aozasa, K., Kawai, T., and Akira, S. (2007). Alveolar macrophages are the primary interferon-alpha producer in pulmonary infection with RNA viruses. Immunity *27*, 240–252.

Kumar, H., Kawai, T., Kato, H., Sato, S., Takahashi, K., Coban, C., Yamamoto, M., Uematsu, S., Ishii, K.J., Takeuchi, O., and Akira, S. (2006). Essential role of IPS-1 in innate immune responses against RNA viruses. J. Exp. Med. *203*, 1795–1803.

Meylan, E., Curran, J., Hofmann, K., Moradpour, D., Binder, M., Bartenschlager, R., and Tschopp, J. (2005). Cardif is an adaptor protein in the RIG-I antiviral pathway and is targeted by hepatitis C virus. Nature *437*, 1167–1172.

Miranda, C., Roccato, E., Raho, G., Pagliardini, S., Pierotti, M.A., and Greco, A. (2006). The TFG protein, involved in oncogenic rearrangements, interacts with TANK and NEMO, two proteins involved in the NF-kappaB pathway. J. Cell. Physiol. *208*, 154–160.

Nakhaei, P., Genin, P., Civas, A., and Hiscott, J. (2009). RIG-I-like receptors: sensing and responding to RNA virus infection. Semin. Immunol. *21*, 215–222.

Onoguchi, K., Yoneyama, M., Takemura, A., Akira, S., Taniguchi, T., Namiki, H., and Fujita, T. (2007). Viral infections activate types I and III interferon genes through a common mechanism. J. Biol. Chem. *282*, 7576–7581.

Oshiumi, H., Matsumoto, M., Hatakeyama, S., and Seya, T. (2009). Riplet/RNF135, a RING finger protein, ubiquitinates RIG-I to promote interferon-beta induction during the early phase of viral infection. J. Biol. Chem. *284*, 807–817.

Pichlmair, A., Schulz, O., Tan, C.P., Naslund, T.I., Liljestrom, P., Weber, F., and Reis e Sousa, C. (2006). RIG-I-mediated antiviral responses to single-stranded RNA bearing 5′-phosphates. Science *314*, 997–1001.

Rehwinkel, J., Tan, C.P., Goubau, D., Schulz, O., Pichlmair, A., Bier, K., Robb, N., Vreede, F., Barclay, W., Fodor, E., and Reis e Sousa, C. (2010). RIG-I detects viral genomic RNA during negative-strand RNA virus infection. Cell *140*, 397–408.

Saito, T., Hirai, R., Loo, Y.M., Owen, D., Johnson, C.L., Sinha, S.C., Akira, S., Fujita, T., and Gale, M., Jr. (2007). Regulation of innate antiviral defenses through a shared repressor domain in RIG-I and LGP2. Proc. Natl. Acad. Sci. USA *104*, 582–587.

Saito, T., Owen, D.M., Jiang, F., Marcotrigiano, J., and Gale, M., Jr. (2008). Innate immunity induced by composition-dependent RIG-I recognition of hepatitis C virus RNA. Nature *454*, 523–527.

Seth, R.B., Sun, L., Ea, C.K., and Chen, Z.J. (2005). Identification and characterization of MAVS, a mitochondrial antiviral signaling protein that activates NF-kappaB and IRF 3. Cell *122*, 669–682.

Shigemoto, T., Kageyama, M., Hirai, R., Zheng, J., Yoneyama, M., and Fujita, T. (2009). Identification of loss of function mutations in human genes encoding RIG-I and MDA5: implications for resistance to type I diabetes. J. Biol. Chem. *284*, 13348–13354.

Sun, Q., Sun, L., Liu, H.H., Chen, X., Seth, R.B., Forman, J., and Chen, Z.J. (2006). The specific and essential role of MAVS in antiviral innate immune responses. Immunity *24*, 633–642.

Suzuki, H., Fukunishi, Y., Kagawa, I., Saito, R., Oda, H., Endo, T., Kondo, S., Bono, H., Okazaki, Y., and Hayashizaki, Y. (2001). Protein-protein interaction panel using mouse full-length cDNAs. Genome Res. *11*, 1758–1765.

Takahasi, K., Yoneyama, M., Nishihori, T., Hirai, R., Kumeta, H., Narita, R., Gale, M., Jr., Inagaki, F., and Fujita, T. (2008). Nonself RNA-sensing mechanism of RIG-I helicase and activation of antiviral immune responses. Mol. Cell *29*, 428–440.

Takeuchi, O., and Akira, S. (2010). Pattern recognition receptors and inflammation. Cell *140*, 805–820.

Xu, L.G., Wang, Y.Y., Han, K.J., Li, L.Y., Zhai, Z., and Shu, H.B. (2005). VISA is an adapter protein required for virus-triggered IFN-beta signaling. Mol. Cell *19*, 727–740.

Yoneyama, M., and Fujita, T. (2009). RNA recognition and signal transduction by RIG-I-like receptors. Immunol. Rev. *227*, 54–65.

Yoneyama, M., and Fujita, T. (2010). Recognition of viral nucleic acids in innate immunity. Rev. Med. Virol. *20*, 4–22.

Yoneyama, M., Kikuchi, M., Natsukawa, T., Shinobu, N., Imaizumi, T., Miyagishi, M., Taira, K., Akira, S., and Fujita, T. (2004). The RNA helicase RIG-I has an essential function in double-stranded RNA-induced innate antiviral responses. Nat. Immunol. *5*, 730–737.

Zeng, W., Sun, L., Jiang, X., Chen, X., Hou, F., Adhikari, A., Xu, M., and Chen, Z.J. (2010). Reconstitution of the RIG-I pathway reveals a signaling role of unanchored polyubiquitin chains in innate immunity. Cell *141*, 315–330.

OPEN ACCESS Freely available online

PLoS one

Hepatitis C Virus Core Protein Abrogates the DDX3 Function That Enhances IPS-1-Mediated IFN-Beta Induction

Hiroyuki Oshiumi[1], Masanori Ikeda[2], Misako Matsumoto[1], Ayako Watanabe[1], Osamu Takeuchi[3], Shizuo Akira[3], Nobuyuki Kato[2], Kunitada Shimotohno[4], Tsukasa Seya[1]*

1 Department of Microbiology and Immunology, Hokkaido University Graduate School of Medicine, Sapporo, Japan, **2** Department of Tumor Virology, Okayama University Graduate School of Medicine, Dentistry, and Pharmaceutical Sciences, Okayama, Japan, **3** Laboratory of Host Defense, WPI Immunology Frontier Research Center, Research Institute for Microbial Diseases, Osaka University, Suita, Japan, **4** Research Institute, Chiba Institute of Technology, Narashino, Japan

Abstract

The DEAD box helicase DDX3 assembles IPS-1 (also called Cardif, MAVS, or VISA) in non-infected human cells where minimal amounts of the RIG-I-like receptor (RLR) protein are expressed. DDX3 C-terminal regions directly bind the IPS-1 CARD-like domain as well as the N-terminal hepatitis C virus (HCV) core protein. DDX3 physically binds viral RNA to form IPS-1-containing spots, that are visible by confocal microscopy. HCV polyU/UC induced IPS-1-mediated interferon (IFN)-beta promoter activation, which was augmented by co-transfected DDX3. DDX3 spots localized near the lipid droplets (LDs) where HCV particles were generated. Here, we report that HCV core protein interferes with DDX3-enhanced IPS-1 signaling in HEK293 cells and in hepatocyte Oc cells. Unlike the DEAD box helicases RIG-I and MDA5, DDX3 was constitutively expressed and colocalized with IPS-1 around mitochondria. In hepatocytes (O cells) with the HCV replicon, however, DDX3/IPS-1-enhanced IFN-beta-induction was largely abrogated even when DDX3 was co-expressed. DDX3 spots barely merged with IPS-1, and partly assembled in the HCV core protein located near the LD in O cells, though in some O cells IPS-1 was diminished or disseminated apart from mitochondria. Expression of DDX3 in replicon-negative or core-less replicon-positive cells failed to cause complex formation or LD association. HCV core protein and DDX3 partially colocalized only in replicon-expressing cells. Since the HCV core protein has been reported to promote HCV replication through binding to DDX3, the core protein appears to switch DDX3 from an IFN-inducing mode to an HCV-replication mode. The results enable us to conclude that HCV infection is promoted by modulating the dual function of DDX3.

Citation: Oshiumi H, Ikeda M, Matsumoto M, Watanabe A, Takeuchi O, et al. (2010) Hepatitis C Virus Core Protein Abrogates the DDX3 Function That Enhances IPS-1-Mediated IFN-Beta Induction. PLoS ONE 5(12): e14258. doi:10.1371/journal.pone.0014258

Editor: Jörn Coers, Duke University Medical Center, United States of America

Received May 28, 2010; **Accepted** November 16, 2010; **Published** December 8, 2010

Funding: This work was supported in part by the Program of Founding Research Centers for Emerging and Reemerging Infectious Diseases, MEXT, Sapporo Biocluster "Bio-S", the Knowledge Cluster Initiative of the MEXT, Grants-in-Aid from the Ministry of Education, Science, and Culture (Specified Project for Advanced Research) and the Ministry of Health, Labor, and Welfare of Japan, Mochida Foundation, Yakult Foundation, NorthTec Foundation and Waxman Foundation. The funders had no role in study design, data collection and analysis, decision to publish, or preparation of the manuscript.

Competing Interests: The authors have declared that no competing interests exist.

* E-mail: seya-tu@pop.med.hokudai.ac.jp

Introduction

The retinoic acid inducible gene-I (RIG-I) and the melanoma differentiation-associated gene 5 (MDA5) encode cytoplasmic RNA helicases [1–3] that signal the presence of viral RNA through the adaptor, IPS-1/Mitochondrial antiviral signaling protein (MAVS)/Caspase recruitment domain (CARD) adaptor inducing interferon (IFN)-beta (Cardif)/Virus-induced signaling adaptor (VISA) to produce IFN-beta [4–7]. IPS-1 is localized to the mitochondrial outer membrane through its C-terminus [6]. Increasing evidence suggests that the DEAD-box RNA helicase DDX3, which is on the X chromosome, participates in the regulation of type I IFN induction by the RIG-I pathway.

DDX3 acts on the IFN-inducing pathway by a complex mechanism. Early studies reported that DDX3 up-regulates IFN-beta induction by interacting with IKKepsilon [8] or TBK1 [9] in a kinase complex. Both TBK1 and IKKepsilon are IRF-3-activating kinases with NF-kappaB- and IFN-inducible properties. DDX3 has been proposed to bind IKKepsilon, and IKKepsilon is generated after NF-kappaB activation [10]. Yeast two-hybrid studies demonstrated that DDX3 binds IPS-1, and both are constitutively present prior to infection (Fig. 1). Ultimately, DDX3 forms a complex with the DEAD-box RNA helicases RIG-I and MDA5 [11], which are present at only low amounts in resting cells, and are up-regulated during virus infection. Previously we used gene silencing and disruption, to show that the main function of DDX3 is to interact with viral RNA and enhance RIG-I signaling upstream of NAP1/TBK1/IKKepsilon [11]. Hence, DDX3 is involved in multiple pathways of RNA sensing and signaling during viral infection.

DDX3 resides in both the nucleus and the cytoplasm [12], and has been implicated in a variety of processes in gene expression regulation, including transcription, splicing, mRNA export, and translation [13]. A recent report suggested that the N-terminus of hepatitis C virus (HCV) core protein binds the C-terminus of DDX3 (Fig. S1) [14,15], and this interaction is required for HCV replication [16]. Although DDX3 promotes efficient HCV infection by accelerating HCV RNA replication, the processes

A

Two representative polyI:C-binding proteins identified by mass-spectrometric analysis

dsRNA-binding protein	ID	Mr (kDa)	polyI:C	polyU	gene name
dsRNA-activated protein kinase	IPI00019463	63 kDa	37	2	PKR
ATP-dependent RNA helicase	IPI00215637	73 kDa	19	12	DDX3

B

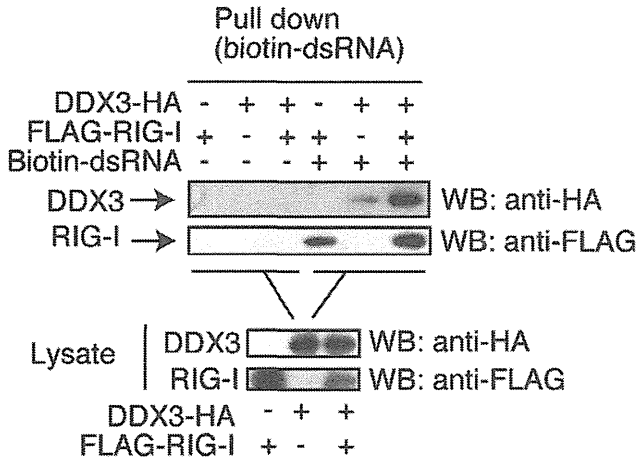

Figure 1. DDX3 is a RNA-binding protein. (A) DDX3 is a polyU- and polyI:C-binding protein. Mass spectrometry analyses indicated that DDX3 binds polyI:C- and polyU-Sepharose, although PKR binds polyI:C but not polyU. The rough data from MASCOT and one representative of six trials are shown. (B) DDX3 binds dsRNA, RIG-I and HCV core protein. Expression vectors for Flag-tagged RIG-I and HA-tagged DDX3 were transfected into HEK293 cells using lipofectamine 2000. Twenty-four hours after the transfection, extract from transfected cells were mixed with biotin-conjugated dsRNA. RNA-protein complex were recovered by pull-down assay using streptavidin-Sepharose. The protein within the pull-down fraction was analyzed by western blotting. The results are representative of two independent experiments.
doi:10.1371/journal.pone.0014258.g001

appear independent of its interaction with the viral core protein [15]. HCV seems to co-opt DDX3, and require DDX3 for replication. In addition, the association between DDX3 and core protein implicates DDX3 in HCV-related hepatocellular carcinoma progression [17]. Therefore, DDX3 could be a novel target for the development of drugs against HCV [18].

A number of reports have demonstrated the formation of the DDX3-core protein complex in the cytoplasm, but the functional relevance of DDX3-core protein interaction is not known. In this report, we show evidence that the HCV core protein participates in suppression of DDX3-augmented IPS-1 signaling for IFN-β induction. Several possible functions of DDX3 are discussed, focusing on its core protein association and IPS-1-regulatory properties.

Materials and Methods

Cell culture and reagents

HEK293 cells and HEK293FT cells were maintained in Dulbecco's Modified Eagle's low or high glucose medium (Invitrogen, Carlsbad, CA) supplemented with 10% heat-inactivated FCS (Invitrogen) and antibiotics. Huh7.5 cells were maintained in MEM (Nissui, Tokyo, Japan) supplemented with 10% heat-inactivated FCS. Hepatocyte sublines with HCV replicon (O cells) and without replicon (Oc cells) were established as described previously [19]. O cells with core-less subgenomic replicon (sO cells) were also generated in Dr. Kato's laboratory [16,19]. RIG-I −/− mouse embryonic fibroblasts (MEF) were gifts from Drs. Takeuchi and Akira [1]. Anti-FLAG M2 monoclonal Ab and anti-HA polyclonal Ab were purchased from Sigma. A mitochondria marker (Mitotracker) and Alexa Fluor®-conjugated secondary antibodies were purchased from Molecular probe. Anti-HCV core mAb (C7-50) [20] and anti-human DDX3 pAb were from Affinity BioReagents, Inc and Abcam, Cambridge MA, respectively.

Plasmids

DDX3 cDNA encoding the entire ORF was cloned into pCR-blunt vector using primers, DDX3N F-Xh (CTC GAG CCA CCA TGA GTC ATG TGG CAG TGG AA) and DDX3C R-Ba (GGA TCC GTT ACC CCA CCA GTC AAC CCC) from human lung cDNA library. To make an expression plasmid, HA tag was fused at the C-terminal end of the full length DDX3 (pEF-BOS DDX3-HA). pEF-BOS DDX3 (1-224aa) vector was made by using primers,

DDX3 N-F-Xh and DDX3D1 (GGA TCC GGC ACA AGC CAT CAA GTC TCT TTT C). pEF-BOS DDX3-HA (225-662) was made by using primers, DDX3D2-3 (CTC GAG CCA CCA TGC AAA CAG GGT CTG GAA AAA C) and DDX3C R-Ba. To make pEF-BOS DDX3-HA (225-484) and pEF-BOS DDX3-HA (485-663), the primers, DDX3D2 R-Ba (GGA TCC AAG GGC CTC TTC TCT ATC CCT C) and DDX3D3 F-Xh (CTC GAG CCA CCA TGC ACC AGT TCC GCT CAG GAA AAA G) were used, respectively. HCV core expressing plasmids, pcDNA3.1 HCVO core or JFH1 core, were previously reported by N. Kato (Okayama University Japan) [16]. Another 1b genotype of the core was cloned from a HCV patient in Osaka Medical Center (Osaka) according to the recommendation of the Ethical Committee in Osaka. We obtained written informed consent from each patient for research use of their samples. Reporter and internal control plasmids for reporter gene assay are previously described [21,22].

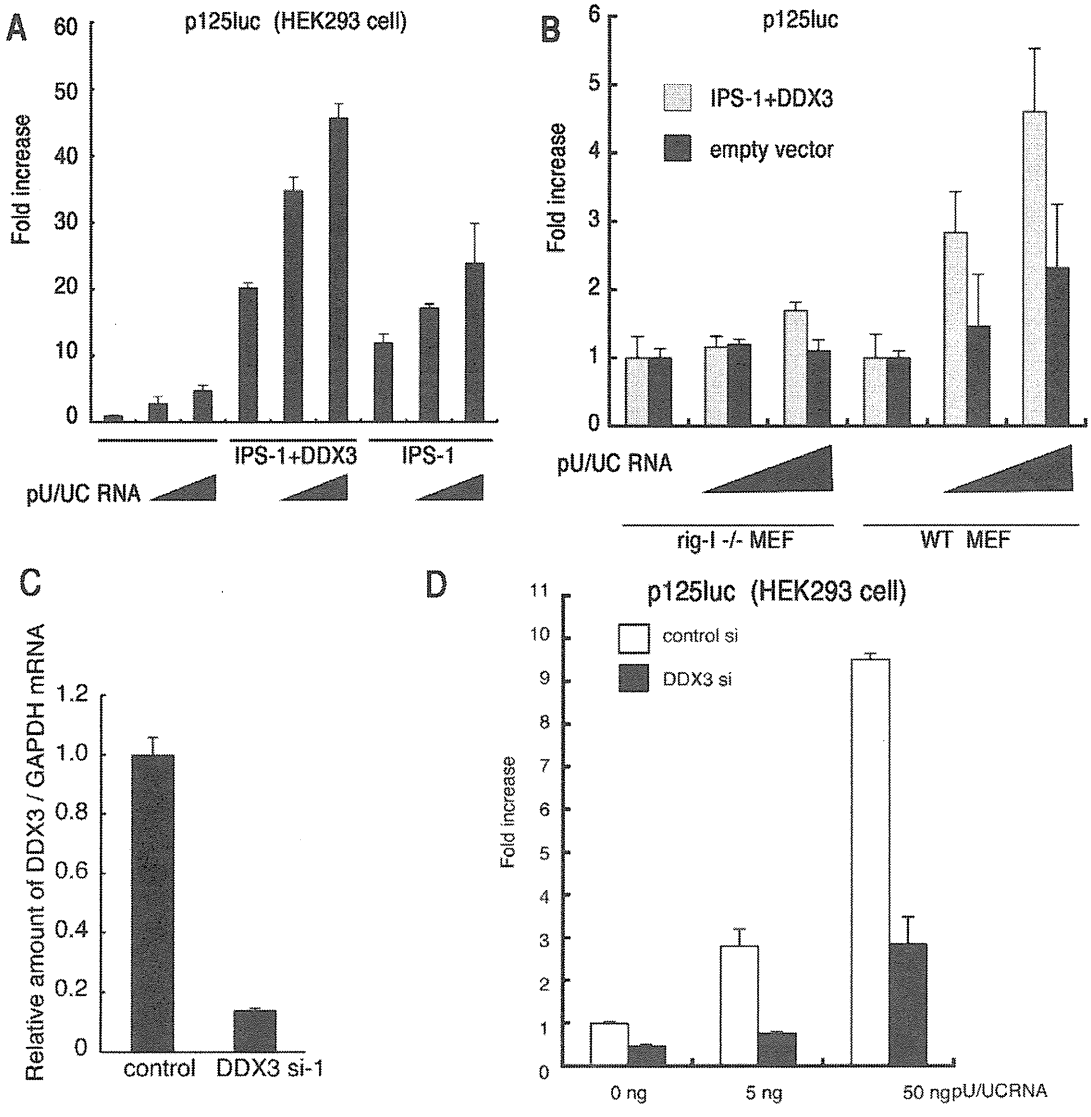

Figure 2. DDX3 is a positive regulator of IPS-1-mediated IFN promoter activation. (A) IFN-β induction by polyU/UC is augmented by DDX3. IPS-1 (100 ng), DDX3 (100 ng) and p125luc reporter (100 ng) plasmids were transfected into HEK293 cells in 24-well plates with or without the HCV 3′ UTR poly U/UC region (PU/UC) RNA (0, 25 or 50 ng/well), synthesized *in vitro* by T7 RNA polymerase. HCV RNA-enhancing activation of IFN-beta promoter was assessed by reporter assay in the presence or absence of the DDX3-IPS-1 complex. (B) RIG-I is essential for the DDX3/IPS-1-mediated IFN-promoter activation. MEF from wild-type and RIG-I −/− mice were transfected with plasmids of IPS-1, DDX3 and p125luc as in panel A, and stimulated with polyU/UC (0, 25 or 50 ng/well). Reporter activity was determined as in panel A. (C) Knockdown of DDX3. Negative control or DDX3 targeting siRNA (20 pmol), DDX3 si-1, was transfected into HEK293 cells, and after 48 hrs, expression of endogenous DDX3 mRNA was examined by real-time RT-PCR. DDX3 si-1-mediated down-regulation of the DDX3 protein was also confirmed by Western blotting (data not shown). (D) DDX3 enhances RIG-I-mediated IFN-beta promoter activation induced by polyU/UC. DDX3 si-1 or control siRNA was transfected into HEK293 cells with reporter plasmids (100 ng). After 48 hrs, cells were stimulated with polyU/UC (5~50 ng/ml) with lipofectamin 2000 reagent for 6 hrs, and activation of the reporter p125luc was measured. The results are representative of at least two independent experiments, each performed in triplicate.
doi:10.1371/journal.pone.0014258.g002

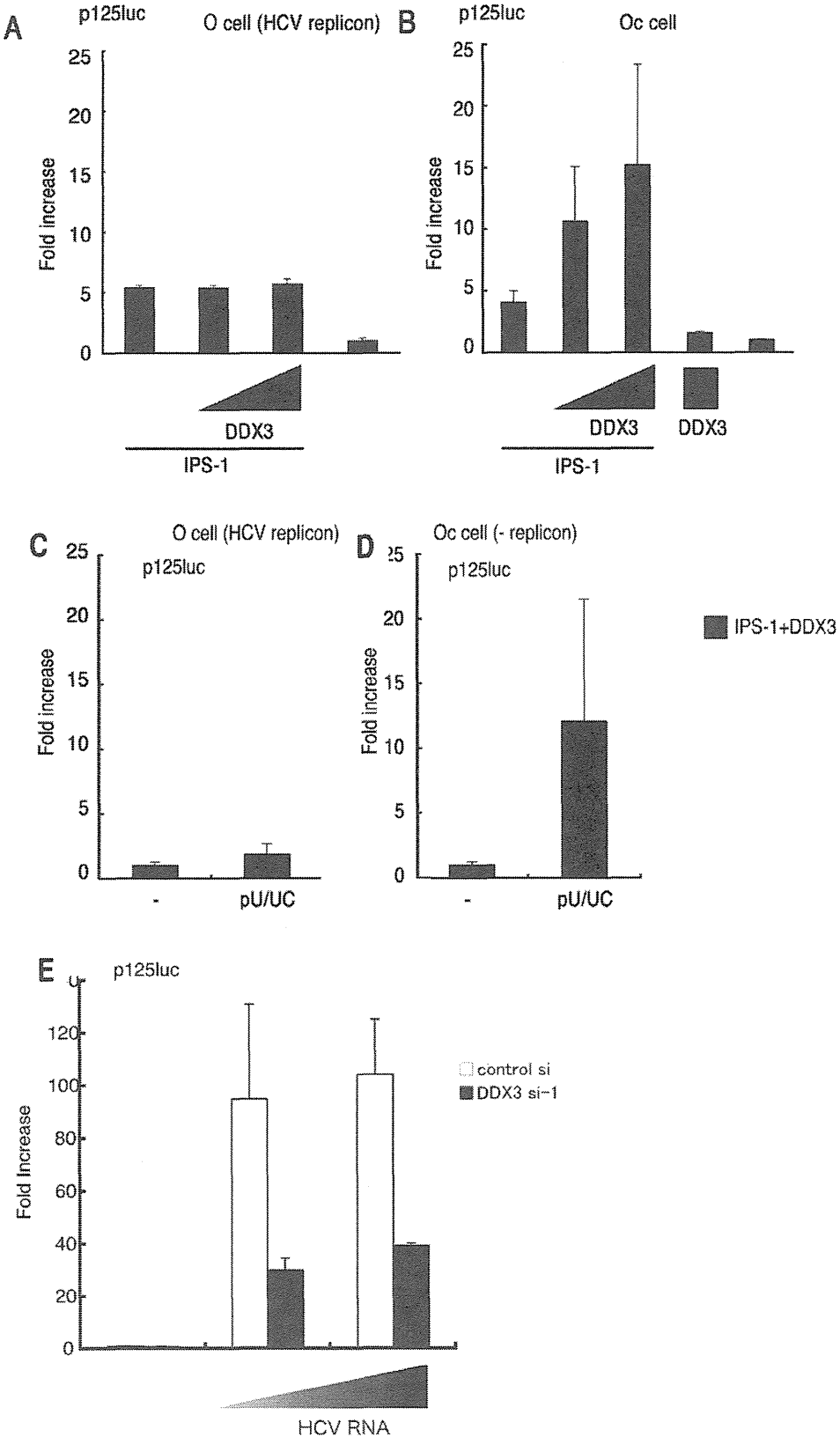
A
p125luc
O cell (HCV replicon)
Fold increase
25
20
15
10
5
0
DDX3
IPS-1
B
p125luc
Oc cell
Fold increase
DDX3
DDX3
IPS-1
C
O cell (HCV replicon)
p125luc
Fold increase
-
pU/UC
D
Oc cell (- replicon)
p125luc
Fold increase
-
pU/UC
IPS-1+DDX3
E
p125luc
Fold Increase
120
100
80
60
40
20
0
control si
DDX3 si-1
HCV RNA

Figure 3. The HCV replicon suppresses IPS-1/DDX3-mediated augmentation of IFN promoter activation. (A,B) O cells with the HCV replicon fail to activate an IFN-β reporter in response to IPS-1/DDX3. O cells contain the full-length HCV replicon, and Oc cells do not [16]. O cells (A) or Oc cells (B) were transfected with IPS-1, DDX3 or p125luc reporter plasmids. At timed intervals (24 hrs), reporter activity was determined as in Fig. 2. (C,D) The HCV replicon suppresses IFN-promoter activation by polyU/UC. O cells and Oc cells expressing IPS-1 and DDX3 were stimulated with polyU/UC. At 48 hrs, reporter activity was determined as in panel A. (E) DDX3 is required for enhanced activation of IFN-beta promoter by O cell HCV 3′UTR. HCV 3′ UTR cDNA was amplified by RT-PCR from RNA extracted from O cells containing full-length HCV replicon. The HCV 3′ UTR RNA was synthesized *in vitro* using T7 RNA polymerase. DDX3 siRNA or control siRNA was transfected into HEK293 cells with the p125luc reporter. After 24 hrs, cells were transfected with HCV RNA, and incubated for 24 hrs. The IFN-beta promoter activation was assessed by luciferase reporter assay. One representative of at least three independent experiments, each performed in triplicate, is shown.
doi:10.1371/journal.pone.0014258.g003

Preparation of HCV polyU/UC RNA

The HCV genotype 1b polyU/UC RNA (from 9421 to 9480, Accession number: EU867431) [23] was synthesized by T7 RNA polymerase *in vitro*. The template dsDNA sequences were; Forward: TAA TAC GAC TCA CTA TAG GGT TCC CTT TTT TTT TTT CTT TTT TTT TTT TTT TTT TTT TTT TTT CTC CTT TTT TTT TC, Reverse: GAA AAA AAA AGG AGA AAA AAA AAA AAA AAA AAA AAA AAA AGA AAA AAA AAA AGG GAA CCC TAT AGT GAG TCG TAT TA. The synthesized RNA was purified by TRIZOL reagent (Invitrogen). cDNA of HCV 3′ UTR region was amplified from total RNA of O cells using primers HCV-F1 and HCV-R1, and then cloned into pGEM-T easy vector. The primer set sequences were HCV-F1: CTC CAG GTG AGA TCA ATA GG and HCV-R1: CGT GAC TAG GGC TAA GAT GG. RNA was synthesized using T7 and SP6 RNA polymerases. Template DNA was digested by DNase I, and RNA was purified using TRIZOL (Invitrogen) according to manufacturer's instructions.

RNAi

Knockdown of DDX3 was carried out using siRNA, DDX3 siRNA-1: 5′-GAU UCG UAG AAU AGU CGA ACA-3′, siRNA-2: 5′-GGA GUG AUU ACG AUG GCA UUG-3′, siRNA-3: 5′-GCC UCA GAU UCG UAG AAU AGU-3′ and control siRNA: 5′-GGG AAG AUC GGG UUA GAC UUC-3′. 20 pmol of each siRNA was transfected into HEK293 cells in 24-well plate with Lipofectamin 2000 according to manufacture's protocol. Knockdown of DDX3 was confirmed 48 hrs after siRNA transfection. Experiments were repeated twice for confirmation of the results.

Reporter assay

HEK293 cells (4×10^4 cells/well) cultured in 24-well plates were transfected with the expression vectors for IPS-1, DDX3 or empty vector together with the reporter plasmid (100 ng/well) and an internal control vector, phRL-TK (Promega) (2.5 ng/well) using FuGENE (Roche) as described previously [23]. The p-125 luc reporter containing the human IFN-beta promoter region (−125 to +19) was provided by Dr. T. Taniguchi (University of Tokyo, Tokyo, Japan). The total amount of DNA (500 ng/well) was kept constant by adding empty vector. After 24 hrs, cells were lysed in lysis buffer (Promega), and the *Firefly* and *Renella* luciferase activities were determined using a dual-luciferase reporter assay kit (Promega). The *Firefly* luciferase activity was normalized by *Renella* luciferase activity and is expressed as the fold stimulation relative to the activity in vector-transfected cells. Experiments were performed three times in duplicate (otherwise indicated in the legends).

PolyI:C or polyU/UC stimulation

PolyI:C was purchased from GE Healthcare company, and solved in milliQ water. For polyI:C treatment, polyI:C was mixed with DEAE-dextran (0.5 mg/ml) (Sigma) in the culture medium, and the cell culture supernatant was replaced with the medium containing polyI:C and DEAE-dextran. Using DEAE-dextran, polyI:C is incorporated into the cytoplasm to activate RIG-I/MDA5.

HCV 3′ UTR poly U/UC region (PU/UC) RNA (0~50 ng/well), which is synthesized *in vitro* by T7 RNA polymerase, transfected into HEK293 cells in 24-well plate by lipofectamin 2000 (Invitrogen) with other plasmids. Cells were allowed to stand for 24~48 hrs and HCV RNA-enhancing activation of IFN-beta promoter was assessed by reporter assay.

Immunoprecipitation (i.p.)

HEK293FT cells were transfected in a 6-well plate with plasmids encoding DDX3, IPS-1, RIG-I or MDA5 as indicated in the figures. 24 hrs after tranfection, the total cell lysate was prepared by lysis buffer (20 mM Tris-HCl [pH 7.5] containing 125 mM NaCl, 1 mM EDTA, 10% Glycerol, 1% NP-40, 30 mM NaF, 5 mM Na_3Vo_4, 20 mM IAA and 2 mM PMSF), and the protein was immunoprecipitated with anti-HA polyclonal (SIGMA) or anti-FLAG M2 monoclonal Ab (SIGMA). The precipitated samples were resolved on SDS-PAGE, blotted onto a nitrocellulose sheet and stained with anti-HA (HA1.1) monoclonal (SIGMA), anti-HA polyclonal or anti-FLAG M2 monoclonal Ab.

Pull-down assay

The pull-down assay was performed according to the method described in Saito T et al. [24]. Briefly, the RNA used for the assay was purchased from JBioS, Co. Ltd (Saitama, Japan). The RNA sequences are (sense strand) AAA CUG AAA GGG AGA AGU GAA AGU G, (antisense strand)CAC UUU CAC UUC UCC CUU UCA GUU U. The biotin is conjugated at U residue at the 3′ end of antisence strand (underlined). Biotinylated double-stranded (ds)RNA were incubated for 1 hr at 25°C with 10 μg of protein from the cytoplasmic fraction of cells that were transfected with Flag-tagged RIG-I and HA-tagged DDX3 expressing vectors. The mixture was transferred into 400 μl of lysis buffer containing 25 μl of streptavidine Sepharose beads, rocked at 4°C for 2 h, collected by centrifugation, washed three times, resuspended in SDS sample buffer.

Proteome analysis of RNA-binding proteins

RNA-binding proteins were identified by affinity chromatography and Mass spectrometry. Briefly, cell lysate was prepared from human HEK293 or Raji cells as will be described elsewhere (Watanabe and Matsumoto, manuscript submitted for publication). The lysate was first applied to polyU-Sepharose and then the pass-through fraction was applied to PolyI:C-Sepharose. The eluted proteins were analyzed on Mass spectrometry using the MASCOT software.

Confocal analysis

HCV replicon-positive (O) or –negative (Oc) cells were plated onto cover glass in a 24-well plate. In the following day, cells were transfected with indicated plasmids using Fugene HD (Roch). The

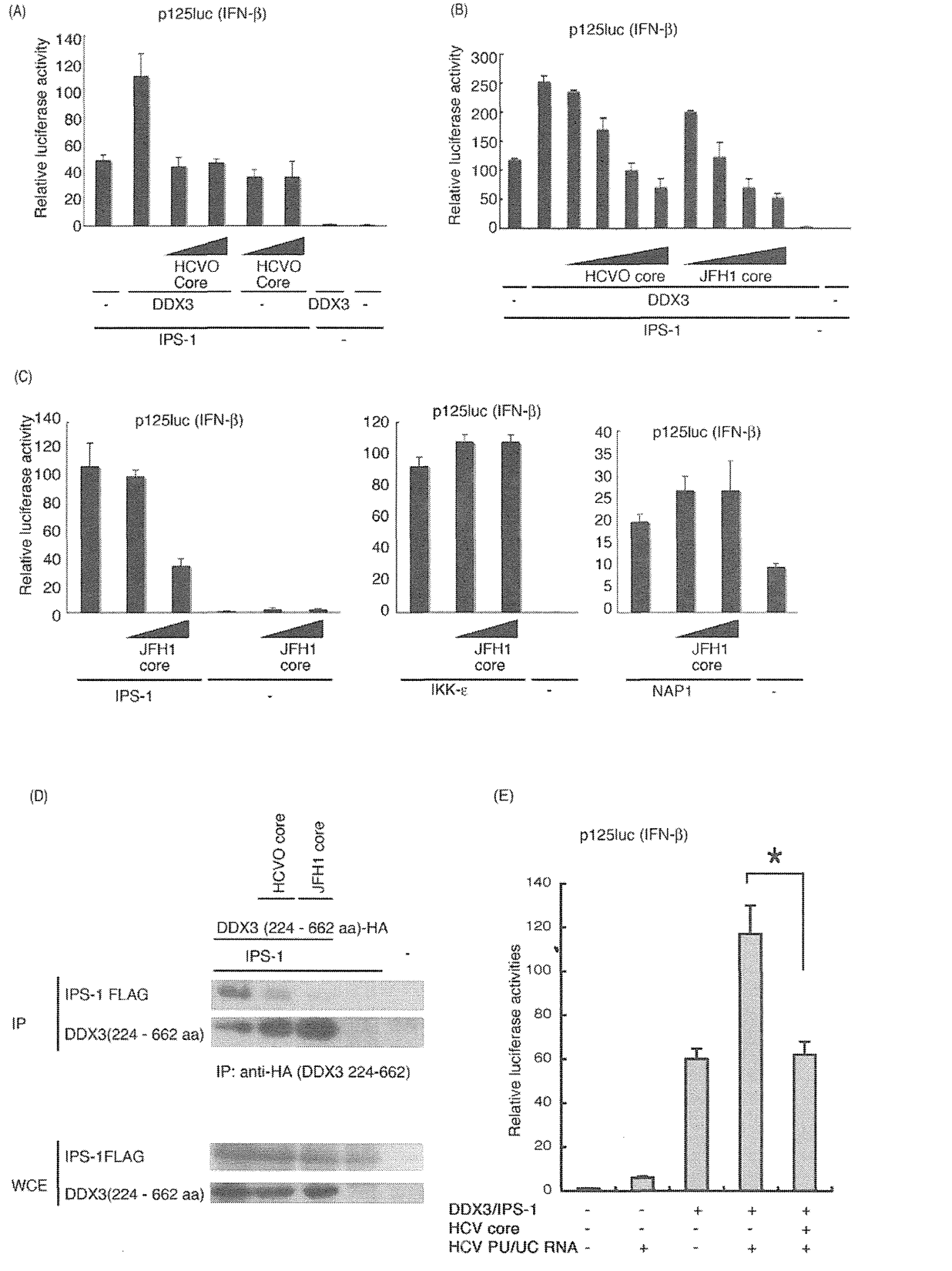
(A)
p125luc (IFN-β)
Relative luciferase activity
HCVO Core
HCVO Core
DDX3
DDX3
IPS-1
(B)
p125luc (IFN-β)
Relative luciferase activity
HCVO core
JFH1 core
DDX3
IPS-1
(C)
p125luc (IFN-β)
Relative luciferase activity
JFH1 core
JFH1 core
IPS-1
p125luc (IFN-β)
JFH1 core
IKK-ε
p125luc (IFN-β)
JFH1 core
NAP1
(D)
HCVO core
JFH1 core
DDX3 (224 - 662 aa)-HA
IPS-1
IP
IPS-1 FLAG
DDX3(224 - 662 aa)
IP: anti-HA (DDX3 224-662)
WCE
IPS-1FLAG
DDX3(224 - 662 aa)
(E)
p125luc (IFN-β)
*
Relative luciferase activities
DDX3/IPS-1
HCV core
HCV PU/UC RNA